Norwegian University of Life Sciences

Master's Thesis 2022 60 ECTS

Faculty of Chemistry, Biotechnology and Food Sciences (KMB)

Establishment of a CD4$^+$ naïve T cell cultivation and stimulation protocol for future studies of cellular responses in rheumatoid arthritis

Emilie Einertsen

Biotechnology – Molecular Biology

Establishment of a $CD4^+$ naïve T cell cultivation and stimulation protocol for future studies of cellular responses in rheumatoid arthritis

Emilie Einertsen

Supervisors:

Dr. Fatima Heinicke
Prof. Benedicte A. Lie
Prof. Harald Carlsen

Oslo University Hospital,
Department of Medical Genetics

and

The Norwegian University of Life Sciences,
Faculty of Chemistry, Biotechnology and Food Sciences

June 2022

2022

Establishment of a $CD4^+$ naïve T cell cultivation and stimulation protocol for future studies of cellular responses in rheumatoid arthritis

Acknowledgements

The work for this thesis was carried out at the Department of Medical Genetics (AMG) at Oslo University Hospital (OUS), from August 2021 to June 2022. The thesis is a part of a Master's Degree in Biotechnology at the Norwegian University of Life Sciences (NMBU), within the Faculty of Chemistry, Biotechnology and Food Sciences.

Firstly, I would especially like to thank Fatima Heinicke for being my main-supervisor and for all her valuable support, encouragement and time devoted to me throughout this thesis, in which I am very grateful. I am also very thankful for my co-supervisor Benedicte A. Lie, for including me in her research group, for all her constructive feedback and advice, and for always being positive and supportive. I am likewise thankful to Siri Tennebø Flåm for devoting so much of her time supervising and helping me in the lab, both during the day and during the night, and for her knowledge and insight into the laboratory work.

I would also like to thank Harald Carlson for being my internal supervisor at NMBU. Additionally, I would like to thank everyone in the immunogenetics group for including me in the group and for the input and good advice along the way.

Lastly, I am grateful for all my loved ones, to all their wonderful support during this last year.

I would also like to give a special thanks to the blood donors at Ullevål blood bank who consented to their buffy coats being used for this research.

Emilie Einertsen

Oslo, May 2022

Sammendrag

Revmatoid artritt (RA) er en kompleks autoimmun sykdom som primært forårsaker leddbetennelser i kroppen. Det er en multifaktoriell sykdom som involverer en kombinasjon av genetiske, epigenetiske og miljømessige faktorer som bidrar til utviklingen av sykdommen, hvorav sigarettrøyking er en av de mest undersøkte miljøfaktorene. RA kan ikke kureres, men pasienter behandles vanligvis med lave doser sykdomsmodifiserende antireumatiske legemidler, som metotreksat (MTX) for å redusere utviklingen av sykdommen.

Patogenesen til sykdommen er fortsatt ikke fullstendig kartlagt, men $CD4^+$ naive T celler antas å være viktige drivere i utviklingen av sykdommen. Målet med denne oppgaven var å optimalisere celledyrkningsprosessen for $CD4^+$ naive T celler i respons til behandling, for å kunne utføre videre forskning på disse cellene. Det ble derfor etablert en optimalisert $CD4^+$ naiv T celle-protokoll for stimulering av celler med MTX og nikotin. For dyrking av T-celler *in vitro,* kan ytterligere stimulering med en CD3/CD28 T celleaktivator være nødvendig for celleproliferasjon og ekspandering. Flowcytometri ble brukt for å undersøke renheten til cellene, hvorav det ble observert at flertallet av de $CD4^+$ naive T cellene utviklet seg til memory/aktiverte celler over tid, og på dag 6 av dyrkningsprosessen var den naive cellepopulasjonen nesten fullstendig borte. Celledyrkningsprotokollen ble derfor forkortet til kun to dager, med behandling av cellene på dag 0 av dyrkningsprosessen og høsting av celler på dag 2.

Den relative celleproliferasjonen til $CD4^+$ T celler med behandling av forskjellige MTX- og nikotinkonsentrasjoner, ble undersøkt ved bruk av WST-1 celleproliferasjonsanalyse. Konsentrasjonene av ytterligere interesse var celler stimulert i 48 timer med 0,005 μM, 0,01 μM og 0,05 μM MTX som ga henholdsvis 100%, 60% og 40% celleproliferasjon. Nikotinkonsentrasjonen av interesse var 10 μM, da celleproliferasjonen ikke ble påvirker og resultater kunne sammenliknes med tidligere forskning utført på $CD8^+$ T celler. Etableringen av denne dyrknings- og stimuleringsprotokollen gjør det mulig å undersøke $CD4^+$ naive T celler i respons til behandling med MTX og eksponering av nikotin i ytterligere detalj.

Abstract

Rheumatoid arthritis (RA) is a complex autoimmune disease that primarily causes inflammation in the synovial membrane of joints in the body. It is a multifactorial disease that involves a combination of genetic, epigenetic, and environmental factors contributing to the progression of the disease, with cigarette smoking being the most well studied environmental risk factors. There is currently no cure for RA, but patients are usually treated with low doses of disease-modifying antirheumatic drugs (DMARDs), such as methotrexate (MTX) in order to slow down the progression of the disease.

The pathogenesis of the disease is still not completely understood, but naïve $CD4^+$ T cells are believed to be important mediators in the development of the disease. The aim of this thesis was to optimize the cell cultivation process of $CD4^+$ naïve T cells in response to treatment, in order to be able to conduct further research on the cells. An optimized $CD4^+$ naïve T cell protocol for stimulation of cells with MTX and nicotine was established. In order to cultivate T cells *in vitro*, additional stimulation with a CD3/CD28 T cell activator is recommended for the cells to expand and proliferate favorably. Flow cytometry was used to monitor the purity of the cells during isolation and shows the majority of the $CD4^+$ naïve cells were observed to develop into memory/activated cells over time, and by day 6 of cultivation the naïve cell population was almost completely lost. The cell cultivation protocol was therefore shortened to only 2 days, with treatment of the cells on day 0 of the cultivation process and harvesting cells on day 2.

The relative cell proliferation of the $CD4^+$ T cells when treated with various MTX and nicotine concentrations were examined using a WST-1 cell proliferating assay. The concentrations of further interest were found to be cells stimulated for 48 hours with 0.005 μM, 0.01 μM and 0.05 μM of MTX giving approximately 100%, 60% and 40% cell proliferation, respectively. The nicotine concentration of interest was 10 μM as it did not affect cell proliferation and it was comparable to previous work carried out on $CD8^+$ T cells. The establishment of this cultivation and stimulation protocol allows for investigating the response of $CD4^+$ naïve T cells to treatment with MTX and exposure to nicotine in further detail.

Abbreviations

APC	Antigen presenting cell
B-lymphocytes	Bone-marrow derived lymphocytes
Cat. No.	Catalog number
cDNA	Complementary DNA
CD*x*	Cluster of differentiation *x*
Conc.	Concentration
DMARD	Disease-modifying antirheumatic drug
DN	Double negative
DP	Double positive
EDTA	Ethylenediaminetetraacetic acid
EtOH	Ethanol
FBS	Fetal bovine serum
FMO	Fluorescence minus one
HLA	Human leukocyte antigen
HLA-I	HLA class I
HLA-II	HLA class II
IL	Interleukin
IL-1	Interleukin-1
IL-10	Interleukin-10
IL-2	Interleukin-2
IL-4	Interleukin-4
IL-6	Interleukin-6
LAF bench	Laminar flow bench
MHC	Major histocompatibility complex
MHC-I	MHC class I
MHC-II	MHC class II
MTX	Methotrexate
PBMC	Peripheral mononuclear cell
PBS	Phosphate-buffered saline
PI	Propidium iodine
RA	Rheumatoid arthritis

RIN	RNA integrity number
RT	Room temperature
SE	Standard error
T-lymphocytes	Thymus derived lymphocytes
TCR	T cell receptor
TGF-β	Transforming growth factor beta
Th*x*	Helper T cell *x*
TNF-α	Tumor necrosis factor alfa
Treg	Regulatory T cell
WST-1	Water-soluble tetrazolium salt

Table of contents

1 Introduction

1.1 Immune system

The immune system is the body's defense against infection. It involves a complex biological network of tissues, cells, and organs, that protects the host from pathogenic microbes and to eliminate toxic substances (1). There are two different types of responses to invasion, called the innate- or the adaptive immune responses. The innate immune response is the body's primary defense against pathogens. It recognizes foreign molecular patterns shared by the pathogens and is activated directly when a given infecting agent is encountered (2). The innate immune response includes a wide range of interacting cells, such as macrophages, mast cells, natural killer cells, monocytes, dendritic cells, neutrophils and eosinophils (3).

The adaptive or the acquired immune response has a memory, and as the name suggests, will continually adapt upon repeated exposure to infecting agents and is therefore highly specific to encountered pathogens (2). An example of this is the immunity that is gained after being vaccinated with a disease-causing agent (3). The adaptive immune response is mainly dependent on a group of white blood cells called lymphocytes. The lymphocytes include two main classes of cells known as bone-marrow derived lymphocytes (B-lymphocytes) and thymus-derived lymphocytes (T-lymphocytes), and both cells express antigen receptors. B-lymphocytes mediate humoral immunity and when differentiating into mature B-cells, secrete antibodies that bind to the pathogens by recognizing specific antigens expressed by the pathogen (2, 4). Antibodies are proteins that circulate the bloodstream of the host until encountered with a foreign antigen. Two of the ways antibodies work is that they will then either block the pathogen's ability to bind to any receptors in the host or mark the pathogens to be eliminated (5). On the other hand, T-lymphocytes mediate cellular immunity and primarily differentiate into either cytotoxic cluster of differentiation 8 ($CD8^+$) T cells that directly kill intracellular pathogens or helper $CD4^+$ T cells that mainly activate other host cells to help eliminate the pathogen (2, 4). T-lymphocytes play an important role in determining and maintaining the host's immune responses and are one of the components that form the immunological memory (6).

1.2 T cells and selection in the thymus

T cells originate from stem cells that reside in the bone marrow, and leave for maturation in the thymus, where they develop from immature T-lymphocytes (thymocytes) to mature T cells (6).

The thymus is an organ that provides a specialized microenvironment that includes stromal cells that provide cytokines and chemokines which are important for the differentiation of T cells (7). In the thymus, the thymocytes will start expressing a receptor for recognition of cell-surface antigens called the T cell receptor (TCR).

The earliest thymocytes do not express CD4 or CD8 and are therefore called double negative (DN) thymocytes. DN thymocytes that express CD25 will go through a process called beta selection, where the cells produce a pre-TCR that forms a complex with CD3 (2, 8). After the thymocytes go through beta selection, the cells will start expressing both CD4 and CD8 co-receptors, making them double positive (DP) thymocytes, while the those that did not go through beta selection will die by apoptosis. The DP thymocytes will go through positive selection in the cortex of the thymus, where the thymocytes with a TCR that has affinity to their ligand, either the major histocompatibility complex (MHC) class I or II, will undergo a positive selection process (8). The function of MHC is to present peptide antigens to the T cells. The MHC class 1 (MHC-I) is recognized by the CD8 co-receptor, and the MHC class II (MHC-II) is recognized by the CD4 co-receptor (5). Thymocytes with weaker affinity to MHC die by apoptosis in the thymus, which applies for more than 95% of the thymocytes, ensuring development of T cells with a functional TCR (2). The positive selection process also determines if the thymocyte will develop into a $CD4^+$ T cell or $CD8^+$ T cell, depending on what MHC they have an affinity for.

After migration to the medulla, the cells then undergo negative selection. Thymocytes that interact too strongly when presented to self-antigens are branded autoreactive cells and will also undergo apoptosis, as they pose a risk for development of autoimmunity. The thymocytes that express low enough affinity can pass the negative selection process and will produce either naïve CD4 or CD8 single positive cells before exiting the thymus and entering the periphery (4, 8). However, in some cases, autoreactive cells will escape the selection process which can potentially lead to development of autoimmune diseases (9).

1.2.1 T cell activation

A functional TCR is a crucial step for the thymocyte to mature into a T cell. Each TCR is unique and has its own specificity for peptide antigens with an affinity to MHC class I or II on the surfaces of antigen precenting cells (APCs) (2). Other immune cells such as dendritic cells, macrophages and B-cells, are examples of APCs (10). The genes that encode for MHC in

humans are called human leukocyte antigens (HLA). There are three main types of molecules in the MHC-I called HLA-A, B and C, which together are termed HLA class I (HLA-I). The main types in the MHC-II complex are called HLA-DP, DQ and DR, called HLA class II (HLA-II) (2). Upon encounter with their specific antigen, the naïve T cells will get activated and differentiate and cannot go back to its naïve phenotype. The differentiated T cells can mediate multiple adaptive immune responses, however, for the T cell to activate and differentiate, three signals are required (Figure 1.1).

The first signal is antigen recognition and occurs when the HLA molecule presenting the antigen peptide, binds to the TCR. As the affinity of the TCR for the HLA molecules on the APC are too low to mediate any interaction between the T cell and the APC, the T cells require co-receptors to mediate a response. Each TCR will either be associated with a CD8 or a CD4 co-receptor that will bind to the different HLA molecules, either HLA-I or HLA-II, depending on the type of co-receptor (11). The second activation signal involves a co-stimulatory signal. Naïve $CD8^+$ T cells receive this signal when the CD40 molecule expressed on an APC interacts with its ligand, CD40L, on the naïve $CD8^+$ T cell (12). Activation of the naïve $CD4^+$ T cell involves CD86 on APCs which interact with the main co-stimulatory molecule CD28, which is expressed on the $CD4^+$ T cells (13). The third signal is cytokine-mediated differentiation and expansion. Cytokines such as interleukin-1 (IL-1), interleukin-6 (IL-6) and tumor necrosis factor (TNF-α) are secreted by the APC and will direct the naïve T cells in differentiating into effector T cells (14, 15).

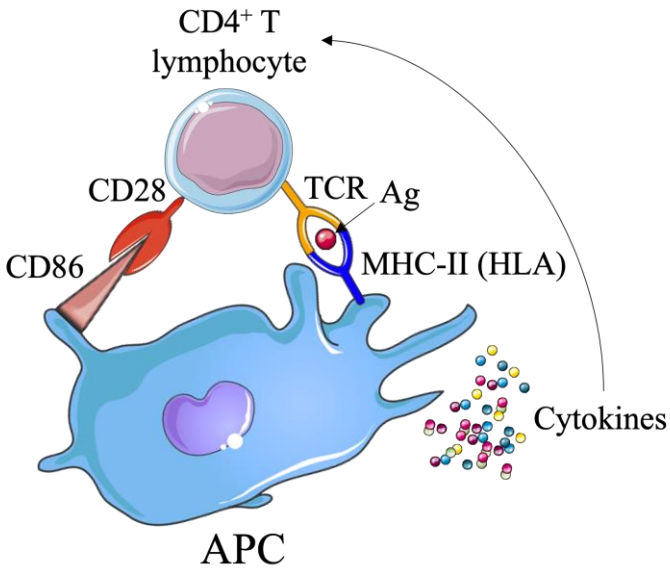

Figure 1.1: Activation of a CD4$^+$ T cell and molecules involved. CD4$^+$ T cell activation involves three signals, where the first signal comes from the interaction between the TCR on the CD4$^+$ lymphocyte and the MHC-II (HLA) and the Ag (antigen) peptide presented by the APC. Second signal involves interaction between the co-stimulatory molecules CD28 on the CD4$^+$ lymphocyte with CD86 expressed on the APC (13). The third signal is cytokines secreted by the APC, taken up by the CD4$^+$ lymphocyte (15). The figure was made with Servier Medical Art by the author, adapted from: (13).

1.2.2 T cell differentiation

After the CD8$^+$ naïve T cells have entered the periphery, the cells will differentiate into effector cells mainly consisting of cytotoxic T cells (16). These cells are capable of directly killing cells infected with a pathogen. After eliminating the infected cells, the majority of the effector cells will undergo apoptosis. However, a small population of the cells will survive long term as memory cells (17).

CD4$^+$ naïve T cells exhibit different functions, such as production of interleukin-2 (IL-2), which promotes development of different T cell subsets. CD4$^+$ naïve T cells will mainly differentiate into helper T cells (Th) that can activate B cells and cytotoxic T cells to help eliminate foreign intruders, while a smaller portion will differentiate into regulatory T cells (Tregs) (2). A fraction of the CD4$^+$ effector T cells will also form an immunological memory and potentially survive long term as memory cells. Memory T cells have the ability to recall previous responses and react quickly to invasion (6). Memory and naïve T cells are often distinguished by the expressions of different isoforms of the CD45 surface molecule. CD45RA is expressed on naïve cells and CD45RO is expressed on memory cells (2).

1.2.3 CD4⁺ T cell subsets

CD4⁺ naïve T cells can differentiate into various subsets of Th effector cells such as Th1, Th2 and Th17, or Tregs, depending on the specific cytokines in their environment (Figure 1.2). Th2 subsets will develop in the presence of interleukin-4 (IL-4) and Tregs in the absence of IL-6 but with the presence of transforming growth factor beta (TGF-β) and IL-2, to mention some (5). The different CD4⁺ T cell subsets can be distinguished by their secretion of different cytokines. The cytokines have many different functions but are all involved in facilitating optimal immune responses against pathogens (18). Th1 and Th2 secrete cytokines that can induce B cells to change what antibody they are producing, while Th17 secrete cytokines to promote inflammatory responses and tissue homeostasis. Tregs mediate immune downregulation by releasing suppressive cytokines such as interleukin-10 (IL-10) and TGF-β, which inhibit other immune cells. The Tregs can be distinguished from the other Th subsets by the expression of surface marker CD25 (13).

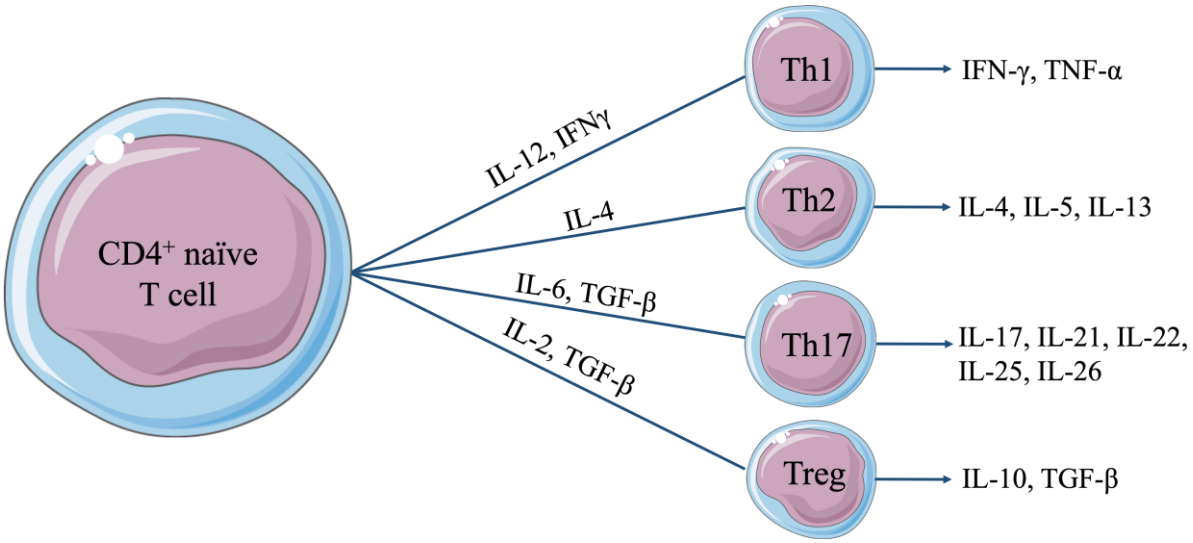

Figure 1.2: A selection of CD4⁺ T cell subsets and cytokines involved. An example selection of different CD4⁺ T cell subsets, however there are more existing subsets. The presence and absence of a variety of cytokines give rise to the different subsets. Each subset is responsible for the production of a group of cytokines with different functions and have their specific roles in immune response. IL = interleukin, IFN-γ = interferon gamma. The figure was made with Servier Medical Art by the author, adapted from: (18).

The number of naïve cells in the body declines after puberty as a result of decreased production of new T cells in the body and more T cells becoming memory cells over time. Since the naïve cells have a role as precursors to all the different T-effector subsets, the decline of these cells has been suggested to contribute to the decline in immune responses in older adults and increased susceptibility to autoimmune diseases (19, 20).

1.3 Autoimmunity and autoimmune diseases

Sometimes T cells start to attack the body's own healthy tissues and cells. This happens due to immune systems failure to distinguish self-antigens from non-self-antigens. When a T cell reacts to an HLA with self-peptides, it will usually not leave the thymus. However, when the T cell is unable to make that distinction, it can cause an immune response towards the host's own cells and tissues. This is the case for patients with autoimmune diseases. There are almost 100 known distinct autoimmune diseases, which together affects about 3-5% of the population (21). Autoimmune diseases can be broadly divided into two main types of disorders. The first being organ specific autoimmune disorders where the autoimmunity is targeted at one specific cell type or tissue. This includes disorders such as multiple sclerosis and type 1 diabetes. The second type of autoimmune disorder is called systemic autoimmune disorder where the immune system attacks self-antigens at multiple sites in the body. The most common types of systemic autoimmune disorders are systemic lupus erythematosus and rheumatoid arthritis (RA) (22).

1.3.1 Rheumatoid arthritis

RA is an autoimmune disease that affects approximately 1% of the population worldwide (23). It primarily causes pain, inflammation and swelling in small joints in the body, specifically the synovial membrane which is the connective tissue that lines the surface of synovial joints, i.e. those joints that allow for movement such as wrists or fingers (23). In the early stages of the disease there are usually only a few joints involved, however as the disease progress more joints are affected, which can result in severe damage, reduced mobility, and loss of function of the joints (24).

It is unknown what triggers RA, but it is thought to be a multifactorial disease, which means a combination of factors are involved (25). There are genetic risk factors involved and, as of early

2022, 101 RA risk loci have been identified (26). The frequency of developing RA is 2 to 3 times higher in women than men (27). The disease most often begins between the ages 40 to 60, however it can occur at any age (28). Other risk factors involve epigenetic and environmental aspects, with cigarette smoking being one of the most studied and well-known environmental factors to increase the risk of developing RA (23). It has actually been reported that exposure to smoking accounts for between 20-30% of the environmental risk for RA (29), and that women who smoke have a 1.3 times higher chance of developing the disease than non-smokers (30). Nicotine, the addictive substance in cigarettes, has been found to exacerbate RA and other inflammatory conditions (31).

The hallmark of RA is synovial inflammation and hyperplasia, meaning increased production of cells in the affected area, leading to swelling. Synovial inflammation and hyperplasia are a result of complex autoimmune and inflammatory processes that involves both the innate and adaptive immune system, and occurs when immune cells such as macrophages, neutrophils and B and T cells, invade the synovial membrane. If RA remains active, this can lead to irreversible joint damages and disabilities (32). Despite the fact that the exact mechanisms leading to the development of the disease are still not fully known, previous studies showed that T cells play a main role in the initiation of the disease (33). Memory/active $CD4^+$ T cells that express CD45RO are found in abundance in the synovial membrane of RA patients and promotes autoantibody formation and contributes to sustain synovial inflammation (34). While T cells in the peripheral blood of RA patients is primarily naïve cells that express the CD45RA. isoform (35). RA used to be considered a Th1-mediated disease, but research suggests that both Th17 and Th22 cells are just as involved (36). Activated naïve $CD4^+$ T cells can differentiate into Th1 and Th17 cells that are both proinflammatory mediators in the progression of the disease. The naïve cells can also differentiate into Th22, that is found in higher frequencies in blood from RA patients although their function is unknown. The inflammatory responses in RA patients also cause naïve T cells to differentiate into atypical T cell phenotypes with lower activation thresholds than naïve cells, which under some circumstances could result in improper autoreactivity (37). In T cell-mediated autoimmune responses, $CD4^+$ T cells are thought to be mediators in the immune response that results in chronic inflammation in patients with autoimmune diseases (38).

1.3.2 Treatment of rheumatoid arthritis with methotrexate (MTX)

There is no cure for RA, however there are treatments used to slow down the progression of the disease and to reduce symptoms. RA is commonly treated with disease-modifying antirheumatic drugs (DMARDs). One of the most commonly used DMARDs is methotrexate (MTX), a small molecule that functions as an anti-inflammatory and immunosuppressive drug. It was originally created as a folic acid antagonist for treatment of various types of cancer, by stopping cells from creating folic acid to make DNA and new cancerous cells. Today RA patients are commonly treated with low-dose MTX over longer periods of time, which causes a decrease in T cell proliferation (39). MTX is found effective in RA patients at concentrations ranging from 15-25 mg weekly, and is often used as monotherapy. However, it can be used as treatment in combination with other types of DMARDs to improve the efficiency of the drugs (39). There have been studies on how smoking can affect the response of DMARDs in RA treatment. One study proposed that RA patients that smoke could need a higher dose of DMARDs, because smoking decrease the effect of the drug (30).

1.4 Culturing of $CD4^+$ T cells *in vitro*

When investigating $CD4^+$ T cells, it is necessary to consider the different components required for the cells to activate and proliferate, which particularly applies when cultivating primary T cells *in vitro*. Optimizing cell culturing processes is essential when studying $CD4^+$ T cells and their potential response to treatment. It can also give increased insight of the cells requirements and provide a good foundation for further analysis.

1.4.1 Restimulation and conditions for T cell cultivation

In our body, the initial activation of the $CD4^+$ T cells happens when the cells interact with the HLA-peptide complex on an APC, which leads to expansion of the $CD4^+$ T cells. This stimulation is antigen-specific but when cultivating the cells *in vitro*, one often wants to stimulate the entire T cell population to promote unbiased expansion and proliferation. Furthermore, in RA, as in most autoimmune diseases, the autoantigen is also unknown. As seen in Section 1.2, an activating signal occurs when the TCR on the $CD4^+$ T cell interacts with the HLA and antigen peptide presented by an APC. However, anti-CD3 antibodies can be used as an alternative to exposing the cells to an antigen, in order to stimulate this activation. The antibody will bind to the TCR-CD3 complex and initiate an activation signal. Research suggests

however, that co-stimulation with CD28 is necessary for the cells to proliferate, and that in the absence of co-stimulation, the T cells can undergo premature apoptosis (40, 41).

The CD28 molecule that is expressed on the $CD4^+$ T cell provides another signal that assists in inducing activation, when it interacts with CD86 expressed on an APC. Prior studies suggested that stimulation with the CD28 molecule when cultivating $CD4^+$ naïve T cells, could assist in the initiation of activating the cells (42). There is also evidence that stimulation with CD2, which is a molecule that binds to CD58 on APCs could also assist in the activation of T cells and in inducing cell proliferation (43). Cell proliferation and IL-2 production was also greatly enhanced by stimulation with CD28, while cells that remained unstimulated had reduced levels of cytokine production and cell proliferation (44). Because of these findings, CD28, CD3 and CD2 are frequently used to stimulate T cells when cultivating and expanding cells *in vitro*.

IL-2 is applied in the cultivation of T cells *in vitro*, due to its immune enhancing functions (45). Originally, the cytokine was called T cell growth factor, because of its ability to enhance T cell proliferation. Research has however shown that IL-2 has many immunostimulatory functions, and promotes T cell growth and differentiation, as well as T cell survival (45).

When expanding T cells *in vitro* there are different media that can be used to provide the appropriate environment for the cells, in combination with IL-2 and the other co-factors mentioned above. One commonly used is the ImmunoCult™-XF T Cell Expansion Media (STEMCELL Technologies, Canada), a serum-free and xeno-free medium that is made specifically for expansion of human T cells from peripheral blood and is optimized for *in vitro* cultivation of T cells. The media contains L-glutamine which is an essential nutrient for the function and expansion of T cells (46). It also contains calcium, which is important for intracellular signaling, and magnesium which has been found to enhance the activation of lymphocytes (47).

1.4.2 Isolating $CD4^+$ T cells

Isolating human $CD4^+$ T cells is a step-by-step process that usually starts with whole blood from healthy donors or patients. The buffy coat is separated from the rest of the blood. The buffy coat consists of granulocytes such as neutrophils, eosinophils and basophils, as well as blood platelets, monocytes and lymphocytes (48, 49). Afterwards, peripheral blood mononuclear cells (PBMCs) are isolated from the buffy coat (Figure 1.3). PBMCs are identified

as blood cells with a round nucleolus and is the part of the buffy coat that includes monocytes and lymphocytes (50). To further isolate specific T cell subsets from the PBMCs, a common method is magnetic activated cell sorting, which is also known as immunomagnetic cell sorting. This process involves magnetic spheres that bind to cells through antibody interactions with specific cell surface markers (51). Cells are then either separated through positive or negative selection. Positive selection is if the cell type of interest is attached to the magnetic beads through corresponding antibodies and the supernatant gets discarded. When a cell type is isolated through negative selection, the undesired cells are attached to the magnetic beads, and the supernatant contains the cells of interest. Negative selection is often preferably used, due to the concern that antibodies that bind to the surfaces of cells of interest might induce unwanted cellular activity (52).

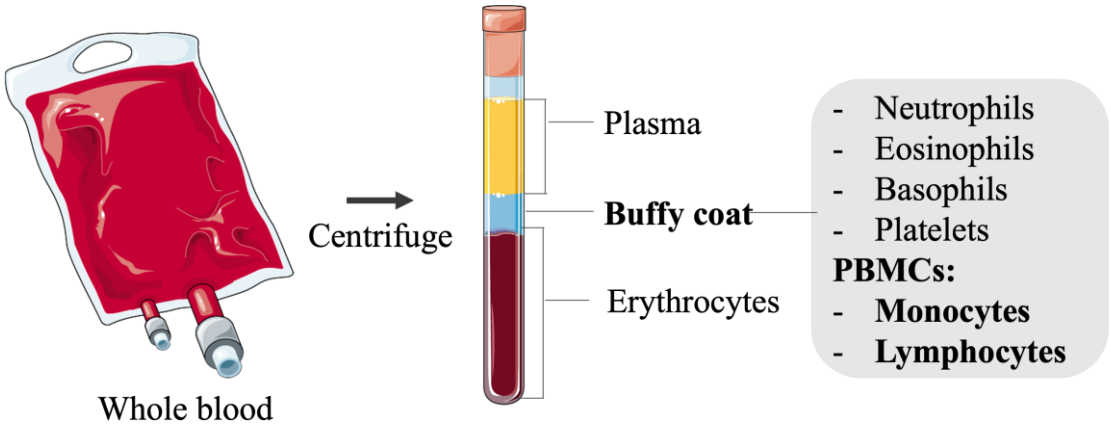

Figure 1.3: Components of whole blood and buffy coat. After centrifugation, whole blood separates into two layers: the top layer is the plasma, and the bottom layer is the red blood cells/erythrocytes. In between is the buffy coat that, among other cells types, consists of the $CD4^+$ T cells, the cell type relevant for this thesis. The figure was made with Servier Medical Art by the author.

1.4.3 Determining cell viability

The viability of the cells should be regularly examined during the cultivation process in order to ensure and determine the health of the cells, and to improve experimental procedures. This can be done by quantifying the amount of viable to non-viable cells in the cell culture. A common and efficient method of assessing viability is using automatic cell counters such as NucleoCounter® NC100™ (ChemoMetec, Denmark) or Countess® II FL (Thermo Fisher Scientific, USA). Automatic cell counters have been shown to be more effective than manual cell counting, when analyzing large sample numbers (53).

The principal reagent of the NucleoCounter® analysis is Reagent A100 (ChemoMetec), added to the cell suspension to lyse the cells, resulting in a suspension with single cell nuclei. This reagent also contains DAPI, which is a fluorescent stain that binds to the nuclei. Then, a second Reagent B (ChemoMetec) is added to the mixture to stabilize the cell nuclei before it is analysed on the NucleoCounter®. When the mixture is loaded on to the instrument, the output given is the total counts of nuclei in the sample (54). On the other hand, the Countess® uses the principle of staining dying/dead cells with Trypan blue to differentiate between viable and non-viable cells. Living cells have intact membranes while in dead or dying cells, the Trypan blue will diffuse through the membrane due to their permeability (53). Flow cytometry can also be used for assessing viability of cells, as well as purity or identification of cells in the sample.

1.4.4 Flow cytometry

Flow cytometry is an instrument used for cell analysis by detecting and measuring the properties of individual cells. Each cell passes through one or more light beams in a flow cytometer, and the amount of light scattered or fluorescence emitted, gives information about the characteristics of the individual cell. The amount of forward scattered light is proportional to the size of the cell and can be used to differentiate between living cells and cellular debris. The amount of side scattered light is proportional to the granular content of the cell and can give information about the cell's complexity. Staining cells with fluorophore-conjugated antibodies that are specific for surface molecules on the cells can be used for detection and quantification of specific cell types (55). Gating in flow can be determined by the fluorescence minus one (FMO) method, where the control cells of the samples are stained with all fluorophores in a panel except one to know where to set the cut-off point of the gating (56). Flow cytometry can be used to assess cell viability by using the Annexin V stain, which detects early apoptotic cells by binding phosphatidylserine, a protein expressed on the cell surface during apoptosis, and is often used in combination with propidium iodine (PI), a fluorescent DNA intercalating agent, to assess the ratio of dead to living cells in a sample (57, 58).

1.4.5 Determining relative cell proliferation using WST-1

Water-soluble tetrazolium salt (WST-1) [2-(4-iodophenyl)-3-(4-nitrophenyl)-5-(2,4-disulfophenyl)-2H tetrazolium monosodium salt] is a stable tetrazolium salt, which is cleaved to a water-soluble formazan dye in metabolic active cells (Figure 1.5) (59). The cleavage causes an absorbance shift due to the reduction of the WST-1 by mitochondrial dehydrogenase

enzymes. The amount of formazan dye produced is directly proportional with the number of living cells in a sample (59, 60). The colorimetric WST-1 assay allows for quick quantification of cell proliferation, growth, and viability in response to treatment, using the cell proliferation reagent WST-1 and a spectrophotometer for quantification.

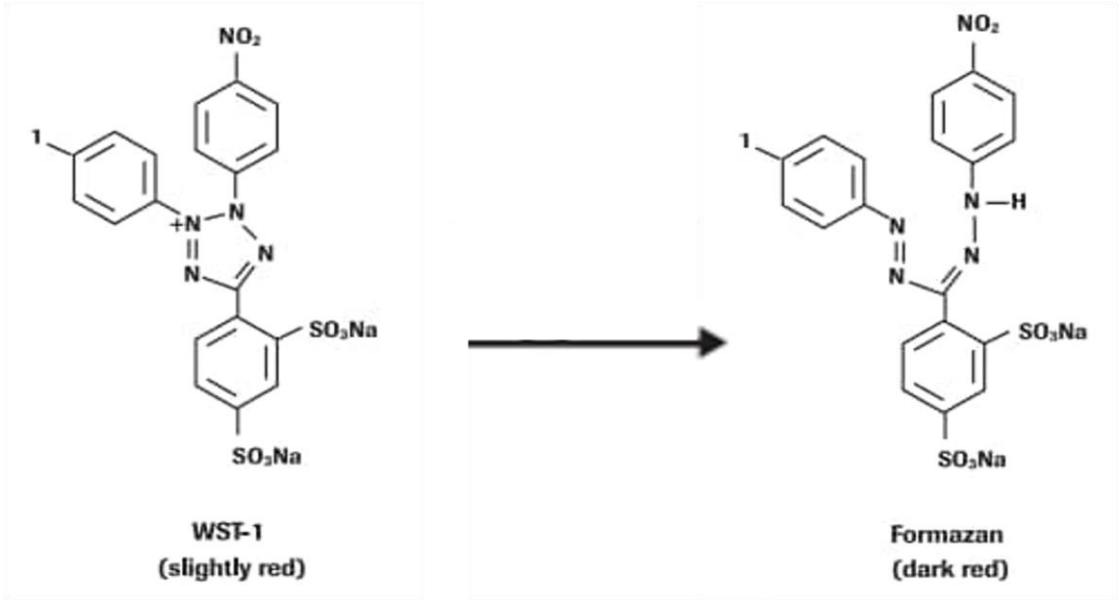

Figure 1.5: Chemical structures of WST-1 and formazan. Tetrazolium salt WST-1 is cleaved to formazan. The sample color turn from slightly red to dark red, depending on the number of living cells in the sample. The figure was obtained from the Sigma-Aldrich Protocol Guide: WST-1 Assay for Cell Proliferation and Viability (61).

2 Aims

The aim of this thesis was to optimize the $CD4^+$ naïve T cell cultivation process to best explore the cellular responses of these cells to treatment. Therefore, the following objectives were investigated:

1. Evaluating activators to provide the best conditions for the viability and expansion of $CD4^+$ naïve T cells.

2. Optimizing the appropriate time frame for cell cultivation.

3. Determining MTX and nicotine concentrations of interest with regards to their influence on relative cell proliferation.

The overall motivation for this thesis is to study $CD4^+$ naïve T cells and their cellular response when treated with MTX or exposed to nicotine, as these are known to affect RA development.

3 Material and methods

3.1 Materials

$CD4^+$ T cells were enriched from buffy coats and a total of nine buffy coats were used (Figure 3.1). The buffy coats were collected from anonymous healthy blood donors provided by the Blood Bank at Oslo University Hospital (OUS), Ullevål, Norway, with ethical approval and informed consent for research. The only information we obtained from the samples was that all donors were within the age group 40-60. Volume of each buffy coat was approximately 50 mL. A complete list of the reagents, kits, equipment, instruments, and software that were used for this thesis is given in appendix I. The experimental overview of the process is presented in the figure below (Figure 3.1).

A

B

Figure 3.1: Experimental overview. The blue captions refer to all the steps that were performed, and the orange captions are the endpoints of all the procedures. (A) Six buffy coats were used to optimize the cell cultivation process and WST-1 assay. (B) Another three buffy coats were used in further analysis after optimizing the protocol.

3.2 Cell culturing environment

In the process of cell cultivation, cells are grown *in vitro* under controlled conditions. All work with cells was performed in a cell culturing laboratory to prevent contamination. The procedures were executed in a sterile laminar flow bench class II (LAF bench), both to reduce contamination and to prevent MTX, which is cytostatic, from being directed at the person working in the bench. Personal protective equipment including clean laboratory coat, gloves and protective sleeves were used. All surfaces of the LAF bench as well as all equipment entering the LAF bench, was sterilised using 70% ethanol (EtOH). Pipette tips, flasks and plates were kept sterile by only opening packaging inside the LAF bench. UV lights were turned on

in the LAF bench every afternoon to sterilise exposed surfaces of the bench. Cells were stored in a CO_2 incubator dedicated to primary cells.

3.2.1 Cell culture conditions

All cells were cultivated in plates or culture flasks in a CO_2 incubator at 37°C with 5% CO_2 humidity. The $CD4^+$ T cells are suspension cells and were passaged by centrifuging the cell suspension and resuspending cells in freshly made media. Cells were cultivated in ImmunoCult™-XF T Cell Expansion Media (STEMCELL Technologies). Human Recombinant IL-2 cytokine (STEMCELL Technologies) was added to the media (5 ng/mL) for T cell growth stimulation. Fresh media, with additional IL-2, was prepared for each cultivation and passaging of cells. Activator (25 mg/mL) was added to media on day 0 to activate T cells and increase T cell expansion.

3.2.2 Determination of activator for cell cultivation

In order to find the activator that maintained the highest viability and best expansion rate for the $CD4^+$ naïve T cells, the cells were incubated with two different activators: ImmunoCult™ Human CD3/CD28 T Cell Activator (STEMCELL Technologies) and ImmunoCult™ Human CD3/CD28/CD2 T Cell Activator (STEMCELL Technologies). 25 µL of activator was added per mL of media used for the cell suspension, on day 0 for all experiments. Cells were divided into two $25cm^2$ Nunc™ Cell Culture Flasks (Thermo Fisher Scientific) and one of the activators was added to each flask. Cell proliferation and viability was assessed after 3 days by observation of cells in a microscope and counting cells using NucleoCounter®. The NucleoCounter® determined number of total- and non-viable cells, and the viability was calculated from these estimates.

3.2.3 Cell morphology and aggregation

The cell morphology, aggregation, proliferation, and possible contamination of cells was examined during the cell cultivation process by visual inspection using a microscope. The cell morphology was compared with the STEMCELL protocol for cultivation of T cells, to ensure the cells had the desired morphology (Figure 3.2) (62). Cell suspension was also inspected for colour changes in media, ensuring the health of the cells.

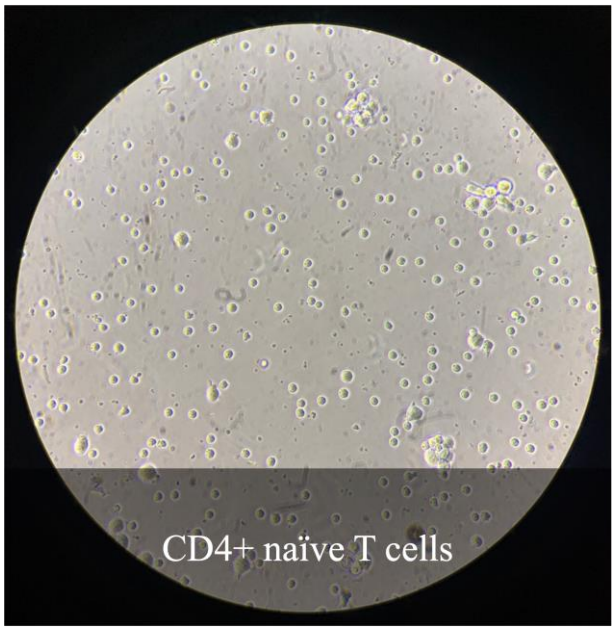

Figure 3.2: Microscopy images of CD4$^+$ naïve T cells. The morphology of the untreated CD4$^+$ naïve T cells was examined at 40x magnification under microscope, on day 3 of cell cultivation.

3.2.4 Cell counts and viability

Cells were counted using primarily the automatic cell counter NucleoCounter® and occasionally also the automatic cell counter Countess® during the cell cultivation process. Countess® was used due to lack of equipment for counting with the NucleoCounter® at certain times, and for confirmation or comparison of unusual counts on the NucleoCounter®. Flow cytometry was used to assess the viability by investigating number of apoptotic cells as well as purity of cell samples. Cells were counted before and after isolation of CD4$^+$ T cells, as well as between every split of cells, and before and after isolation of CD4$^+$ naïve T cells.

The first step of determining the cell count using the NucleoCounter®, was finding the total cell concentration. This was done by mixing 100 µL of the cell suspension with Reagent A100 (ChemoMetec, Denmark) 1:1 in a 1.5 mL Eppendorf tube and then vortexing the mixture. Reagent B (ChemoMetec) was added to the mixture, 1:1:1, and again vortexed to a homogenous suspension. The mixture was loaded onto a NucleoCassette™ (ChemoMetec) and placed in the NucleoCounter®. The second step was determining the concentration of non-viable cells in the sample. Undiluted cell suspension was loaded onto the NucleoCassette™ and placed in the NucleoCounter®. The viability of the cells was then calculated using the equation (3.1) acquired from the NucleoCounter® User's Guide (ChemoMetec):

$$\%Viability = \frac{C_t \times M_t - C_{nv} \times M_{nv}}{C_t \times M_t} \times 100\% \quad (3.1)$$

%Viability: The percentage of viable cells in the cell suspension.

C_t: The total concentration of cells in the NucleoCassette (the displayed result of the total cell count).

C_{nv}: The concentration of non-viable cells in the NucleoCassette (the result displayed when counting the non-viable cells).

M_t: The multiplication factor used for the total cell count.

M_{nv}: The multiplication factor used for the counting of non-viable cells (most often 1).

When using Countess®, 10 µL of cell suspension was mixed with 10 µL of 0.4% Trypan Blue stain (Thermo Fisher Scientific) in a 1.5 mL tube. 10 µL of the mixture was loaded onto a Countess™ Cell Counting Chamber Slide (Thermo Fisher Scientific) and loaded onto the instrument. The results of the counts were presented on the instrument as the total-, viable- and non-viable cell counts and the viability (%) of cells in the sample.

3.2.5 Flow cytometry and fluorescent staining of cells

Flow cytometry was used to examine the purity and viability of the $CD4^+$ T cells and to inspect the T cell phenotypes, including memory to naïve ratio of the cells during the cell cultivation process. The $CD4^+$ T cells and the naïve subtype were analyzed using the BD Accuri™ C6 Plus Personal Flow Cytometer (BD Biosciences, USA) and the BD Accuri™ C6 Plus Software (BD Biosciences). The flow cytometer was analyzing the cell samples until 20,000 events were acquired, however in some cases there were less than 20,000 events, and the instrument was then allowed to run until the whole sample was analyzed.

Cells were collected from cell suspension and centrifuged at 340g for 10 minutes at room temperature (RT). The supernatant containing the media was discarded and the cell pellet was resuspended in 489 mL Phosphate-buffered saline (PBS) (without Mg/Ca) (Thermo Fisher Scientific), with 1 mL Ethylenediaminetetraacetic acid (EDTA) (0.5M, pH = 8) (Thermo Fisher Scientific) and 10 mL fetal bovine serum (FBS) (BIOWEST, France). The cell suspension was divided into 5 mL Polypropylene round-bottom tubes (BD Biosciences) with 100 µL suspension of approximately $1x10^5$ cells in each tube. 10 µL of γ-globulin (4 mg/mL) (Sigma-Aldrich, USA) was added to all samples except samples for autofluorescence and viability, then incubated for 15 minutes at 4°C. 2 µL (15 µL of the CD3-PE antibody) of the fluorophore conjugated antibodies for target markers were added to the cell samples and incubated for 30

minutes. A full list of antibodies used is presented in the table below (Table 3.1). The antibodies added was for examining purity were CD4, CD3, CD8/CD68 and for naïve/memory cell ratio; CD4, CD45RA, CD45RO. The antibody CD68 was used to investigate possible monocytes in the samples. Cells were then washed with 1 mL of PBS, centrifuged at 1500g for 5 minutes and the supernatant was discarded. Gating for cell populations were set according to FMO of control/untreated cell samples for purity (CD4, CD3, CD8) and for naïve/memory ratio (CD4, CD45RA, CD45RO).

For analysis of viability and autofluorescence, 50 μL of cell suspension of approximately $5x10^4$ cells was added to each tube. To examine possible apoptosis of the cells, 50 μL of 1xAnnexin V buffer (1xAnnexin V buffer was made by adding 5 μL of 10xAnnexin V binding buffer (BD Biosciences) with 45 μL of Nuclease-Free Water (Qiagen, Germany) and 5 μL of Annexin V-FITC (Cat. No. 556419, BD Biosciences) were added to cell sample and incubated for 30 minutes at 4°C. Cell sample(s) for measuring autofluorescence were left untreated without any antibodies. Both samples for autofluorescence and viability were left unwashed before being analyzed using the flow cytometer.

Table 3.1: Fluorophore conjugated antibodies used for extracellular flow cytometry analysis.

Antibody/Target	Fluorophore	Clone	Isotype	Source	Cat. No.	Conc. (µg/mL)	Amount used**
CD4	FITC	A161A1	Rat IgG2b	Nordic Biosite (BioLegend®)	357406	50	2 µL
CD3	PE	SK7	Mouse IgG1	Nordic Biosite (BioLegend®)	344806	6.25	15 µL
CD8	APC	SK1	Mouse IgG1	Nordic Biosite (BioLegend®)	344722	25	2 µL
CD45RA	APC	HI100	Mouse IgG2b	Nordic Biosite (BioLegend®)	304112	6	2 µL
CD45RO	PE	UCHL1	Mouse IgG2a	Nordic Biosite (BioLegend®)	304206	40	2 µL
CD45RO	FITC	UCHL1	Mouse IgG2a	Nordic Biosite (BioLegend®)	304204	100	2 µL
CD68*	APC	Unknown	Unknown	Nordic Biosite (BioLegend®)	Unknown	Unknown	2 µL

*This reagent was kindly borrowed from the Department of Immunology at Rikshospitalet, and unfortunately it was not possible to locate all information about it.

** Same amount was used for all assays

3.3 $CD4^+$ T cell isolation process

To investigate the effects of MTX and nicotine on $CD4^+$ naïve T cells, PBMCs were separated from buffy coats from the blood of healthy blood donors and $CD4^+$ T cells were isolated from the PBMCs.

3.3.1 Isolation of PBMCs

To investigate the effects of MTX and nicotine on $CD4^+$ naïve T cells, PBMCs were separated from buffy coats from the blood of healthy blood donors and $CD4^+$ T cells were isolated from the PBMCs. PBMCs were isolated by density gradient centrifugation (Figure 3.3). An isolation buffer was made from 489 mL PBS (without Mg/Ca), 1 mL EDTA (0.5M, pH = 8) and 10 mL FBS. A PBMC wash buffer was prepared using 498 mL PBS and 2 mL EDTA (0.5M, pH = 8). 50 mL of buffy coat was divided into two 50 mL Sarstedt tubes, 25 mL in each tube. 25 mL of isolation buffer was added to each tube and mixed gently by hand. 13 mL of the density gradient liquid Lymphoprep™ (STEMCELL Technologies) was added to three 50 mL SepMate™ tubes (STEMCELL Technologies). 33 mL of the buffy coat and isolation buffer mixture was added to each SepMate tube. Tubes were centrifuged at 1200g for 10 minutes at RT to separate the PBMCs from the red blood cells, platelets, and the granulocytes. The PBMC suspension were transferred to four new 50 mL Sarsted tubes, 25 mL in each and diluted 1:1 with the wash buffer. Tubes were then centrifuged at 340g for 10 minutes at RT. The supernatant was removed, and the cells were carefully resuspended in a total of 7 mL of isolation buffer. Samples from the four tubes were pooled together into one tube and counted using NucleoCounter®.

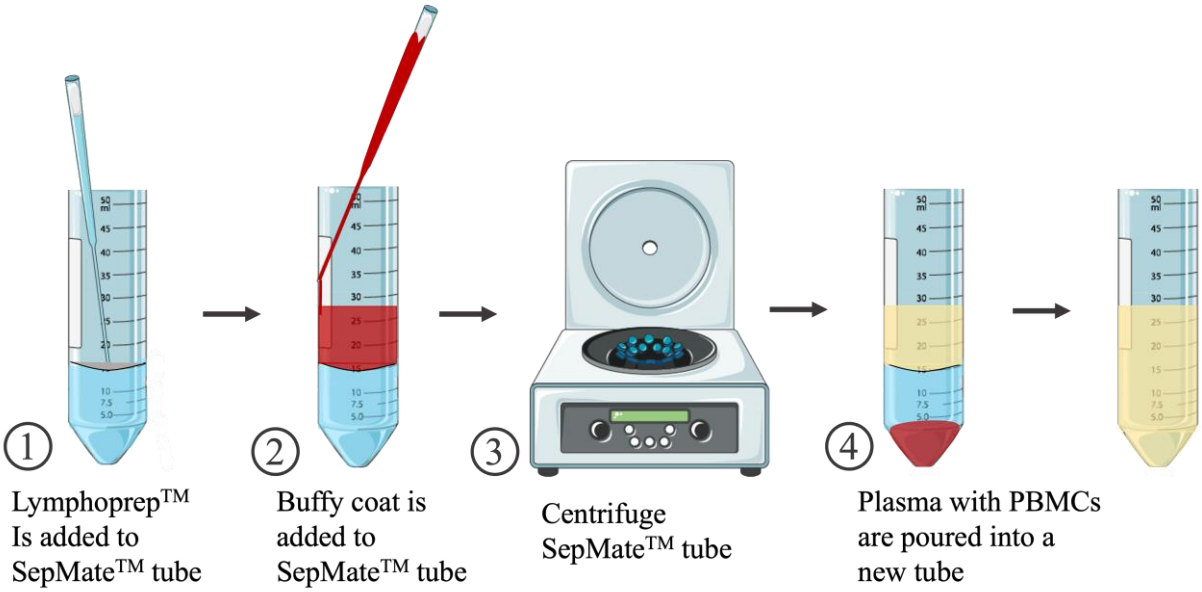

Figure 3.3: Isolation of PBCSs from buffy coat. Experimental overview of PBMCs being isolated from the buffy coat. Lymphoprep™ is added to a SepMate™ tube with the buffy coat, and sample is centrifuged for 10 minutes. The red blood cells and Lymphoprep™ sediment at the bottom of the tube and the plasma with PBMCs on top of the tube, is poured into a new tube. The figure was made with Servier Medical Art by the author.

3.3.2 CD4⁺ T cell isolation

CD4⁺ T cells were isolated through immunomagnetic negative selection using the EasySep™ Human CD4⁺ T Cell Isolation Kit (STEMCELL Technologies). A schematic illustration of the procedure is presented in the figure below (Figure 3.4). $4x10^8$ of the isolated PBMCs were transferred to a 14 mL polystyrene round-bottom tube (BD Biosciences) and centrifuged at 340g for 10 minutes at RT, and the supernatant was removed. The pellet of cells was resuspended in 8 mL of the isolation buffer as previously described in 3.3.1, giving a concentration of $5x10^7$ cells/mL. 400 µL of the antibody EasySep™ Human CD4⁺ T Cell Isolation Cocktail was added to the cell suspension, resuspended by carefully pipetting suspension up and down 10 times and incubated for 5 minutes at RT. The magnetic beads EasySep™ Dextran RapidSpheres™ were vortexed for 30 seconds and 400 µL were added to the cell suspension. An additional 1.2 mL of media was added to the cell suspension giving a total suspension of 10 mL and the mixture was resuspended. The cell suspension was then incubated without the lid, on a EasySep™ magnet (STEMCELL Technologies) for 3 minutes. The supernatant with the CD4⁺ T cells was then poured from the tube, while still on the magnet, into a 50 mL Sarstedt tube or a new 14 mL polystyrene tube if the naïve cells were to be enriched for, consecutively. Undesired cells remained with the magnetic spheres in the tube on the

magnet. The CD4$^+$ T cells were then centrifuged and resuspended in freshly made ImmunoCult™-XF T Cell Expansion Media containing IL-2 and activator as previously described in 3.2.1.

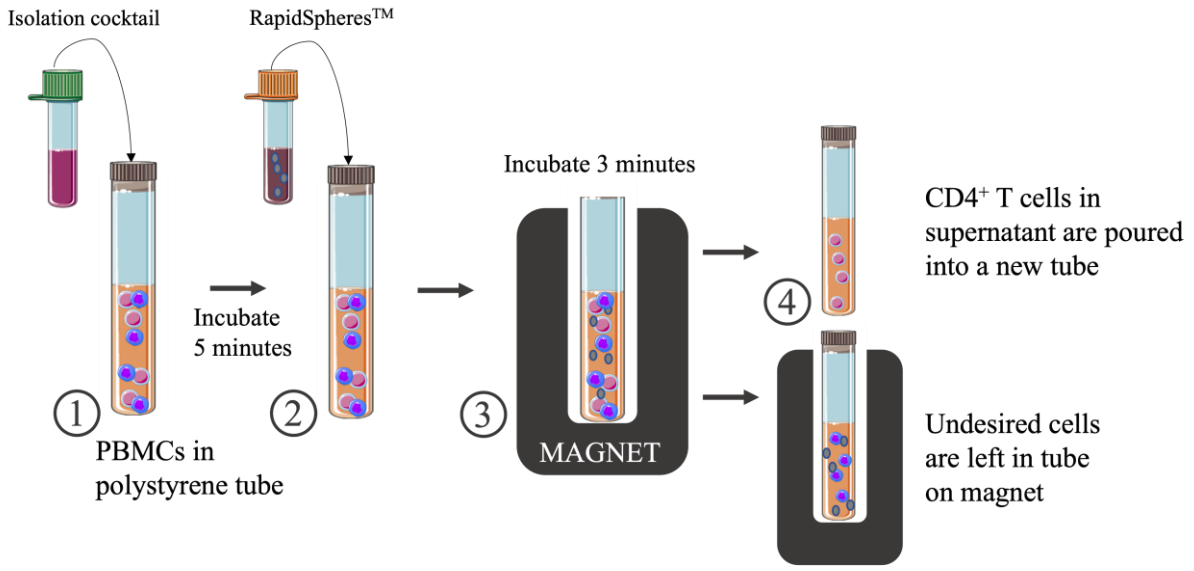

Figure 3.4: Isolation of CD4$^+$ T cells by immunomagnetic negative selection. Schematic illustration of CD4$^+$ T cells being isolated by addition of EasySep™ Human CD4$^+$ T Cell Isolation Cocktail and EasySep™ Dextran RapidSpheres™, and incubation on EasySep™ magnet. CD4$^+$ T cells remaining in the supernatant were poured from the magnet into a new tube. The figure was made with Servier Medical Art by the author.

3.4 WST-1 assay

WST-1 was used to assess relative cell proliferation of CD4$^+$ T cells upon treatment with different concentrations of MTX and nicotine and to find the optimal treatment conditions for further analysis. Relative cell proliferation is measured by addition of the WST-1 cell proliferating reagent that produces a formazan-dye which absorbance is directly proportional to number of living cells in the sample.

3.4.1 Incubation with concentrations of MTX and nicotine prior to WST-1 assay

A stock of MTX (220 µM) was made from MTX Ebetrex (220.6 mM/100 mg/mL) (EBEWE Pharma, Austria), diluted in ImmunoCult™-XF T Cell Expansion Media. The stock was made fresh for every experiment. Additionally, a stock of nicotine (308.5 µM) was made from nicotine (6170 mM/1g/mL) (Sigma-Aldrich), diluted in ethanol (EtOH) (100%). The nicotine stock was kept at 4°C, during the cultivation process for all experiments. CD4$^+$ T cells were

seeded out in Nunc^{TM} 96-Well Microplates (Thermo Fisher Scientific) with a concentration of $5x10^5$ cells/mL. The total volume of cell suspension for each well varied between 200-280 µL, depending on the experiment. Cells were treated with various concentrations of MTX ranging between 0.001 and 5 µM or with nicotine ranging between 1 and 20 µM and were incubated for 24h and 48h depending on the experiment. All concentrations of MTX and nicotine are illustrated in the figure below (Figure 3.6). Mock concentrations were also made for each concentration of MTX and nicotine, with additional EtOH-media or media substituting the concentrations of MTX and nicotine. Wells without cells, but with or without additional MTX and nicotine was also included. Replicates for each concentration was between 2-6 depending on the experiment. To reduce evaporation from the wells during the incubation time, 200 µM of PBS was added to all wells surrounding wells of interest. The plate set-ups for both the MTX and nicotine experiments are presented in appendix II. After incubation with the different treatments and before the WST-1 assay was conducted, small samples were harvested from the wells for flow cytometry analysis.

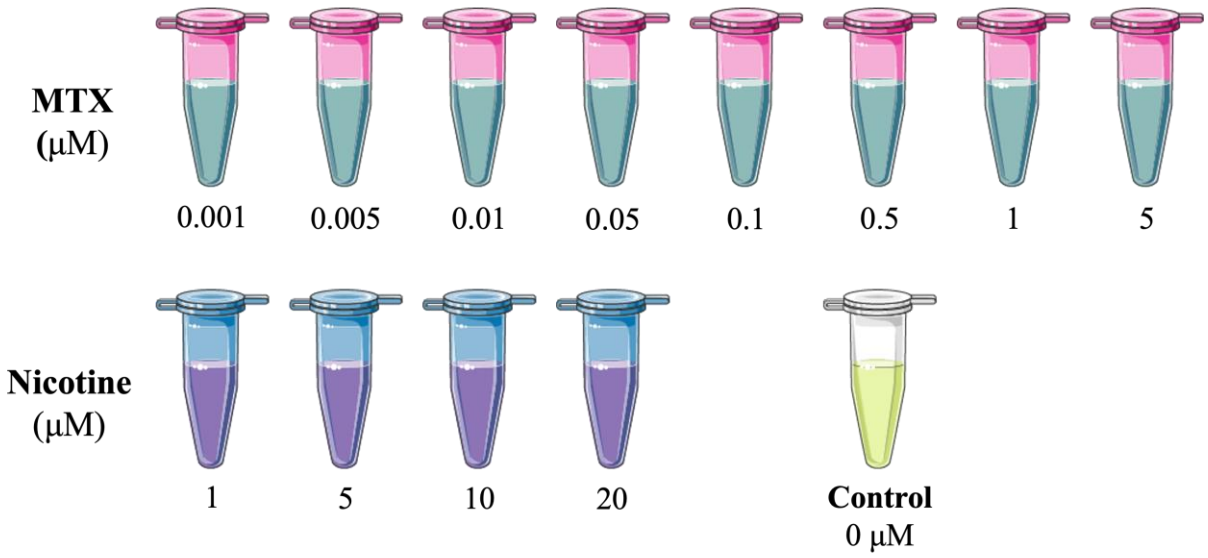

Figure 3.6: Concentrations (µM) of MTX and nicotine tested on CD4$^+$ T cells. Cells were treated with different concentrations (µM) of MTX and nicotine after isolation of CD4$^+$ T cells. A control without any treatment or additional EtOH or media was also included. The figure was made with Servier Medical Art by the author.

3.4.2 WST-1 and spectrophotometer read procedure

The WST-1 assay procedure is illustrated in the figure below (Figure 3.7). After incubation with MTX and nicotine, the Cell Proliferation Reagent WST-1 (Roche Diagnostics, Germany)

was added to each well. The ratio of cell suspension to WST-1 added was 1:10, with 20 µL of WST-1 added to 200 µL of cell suspension. The plates were read on the spectrophotometer VersaMax Microplate Reader (Molecular Devices, USA) and absorbance was measured at 450 nm with a reference wavelength of 745 nm. Absorbance was read at multiple incubation timepoints from 0.5-4 hours. In between timepoints the plates were incubated in darkness, at 37°C. The plates were vortexed for approximately 30 seconds prior to every measurement being taken on the spectrophotometer. The output was analyzed by transferring the raw data from software SoftMax Pro 6.4 (Molecular Devices) to Excel (Microsoft, USA) and relative cell proliferation for $CD4^+$ T cells with each sample treatment was calculated using the equation:

$$\%Proliferation = \frac{Sample - mean(C_{neg})}{mean(C_{pos}) - mean(C_{neg})} \times 100\% \qquad (3.2)$$

%Proliferation: Percentage of relative cell proliferation for each well

Sample: The sample of interest (cells + medium + treatment)

C_{neg}: Negative control (medium + treatment – no cells)

C_{pos}: Positive control (cells + medium – no treatment)

Graphpad Prism 9 (Graphpad Software Inc, USA) was used for visualization of data acquired from the spectrophotometer read.

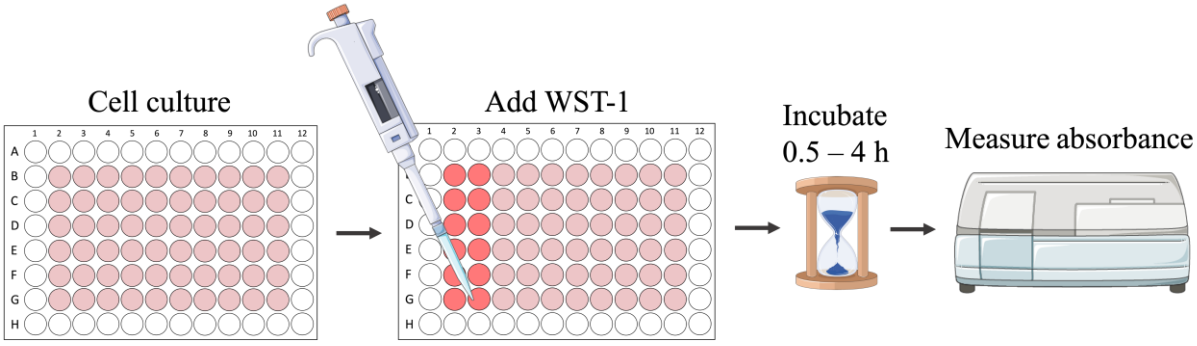

Figure 3.7: Schematic illustration of the WST-1 assay procedure. Cells were cultured in 96-well plates, and WST-1 was added to each well. Plates were incubated at 37°C in the dark for 0.5 to 4 hours, and absorbance was measured on a spectrophotometer at several timepoints during this time. The figure was made with Servier Medical Art by the author.

3.4.3 Final treatments used for further analysis

Based on the results from the former WST-1 experiments, $CD4^+$ T cells were isolated from three new buffy coats and treated with eight different conditions. The treatment conditions are listed in the figure below (Figure 3.8). All cell samples were incubated with the different treatment conditions for 48 hours before the naïve subgroup was isolated.

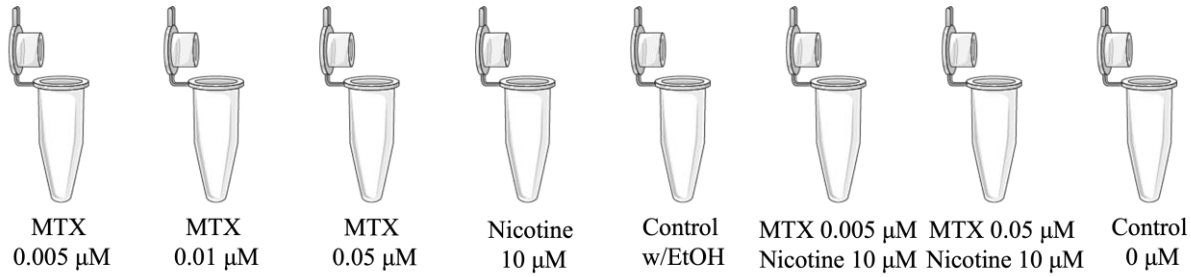

Figure 3.8: Treatments for $CD4^+$ T cells before isolation of naïve subgroup and RNA extraction. Cells were treated with different conditions for 48 hours prior to being depleted for $CD25^+$ T cells and isolated into $CD4^+$ naïve T cells. The figure was made with Servier Medical Art by the author.

3.5 Isolation of naïve subgroup from treated $CD4^+$ T cells

The naive cells were isolated immediately after $CD4^+$ T cell isolation on day 0 for the first three experiments used during the optimization of the $CD4^+$ T cell cultivation procedure. For the three experiments used for further analysis, the naïve cells were isolated as a last step of cell cultivation, after being stimulated with MTX and nicotine (Figure 3.1). Before isolating the naïve subgroup, $CD4^+$ T cells were depleted for $CD25^+$ T cells.

3.5.1 Depletion of $CD25^+$ T cells from $CD4^+$ T cell suspension

$CD25^+$ T cells were depleted from the $CD4^+$ T cells by immunomagnetic negative selection using the EasySep™ Human Pan-CD25 Positive Selection and Depletion Kit (STEMCELL Technologies). $1x10^8$ cells in 1 mL of suspension was added to a 14 mL polystyrene tube. For cell numbers that were under $1x10^7$, suspension volume was at 100 µL and volume of reagents added was recalculated. 1 mL of cell suspension was combined with 50 µL of EasySep™ Pan-CD25 Positive Selection and Depletion Cocktail, mixed and incubated for 10 minutes at RT. EasySep™ Dextran RapidSpheres™ was vortexed for 30 seconds and 100 µL were added to the cells and incubated for 3 minutes at RT. Isolation buffer was added to the mixture to reach a total of 2.5 mL, and the cells were incubated on a magnet for 3 minutes. The $CD4^+$ T cells depleted for $CD25^+$ T cells were poured while still on the magnet, into a new 14 mL

polystyrene tube. Wash step was repeated four times for half of the experiments, due to lower purity observed in flow analysis.

3.5.2 Isolation of $CD4^+$ naïve T cells

$CD4^+$ T cells were subtyped into naïve cells by immunomagnetic negative selection using the EasySep™ Human PE Positive Selection Kit II (STEMCELL Technologies) together with the PE anti-human CD45RO Antibody (Cat. No. 304206, BioLegend®, USA). Information about the antibody, is listed in the table above of antibodies used for flow cytometry (Table 3.1). The volume of each of the reagents added was based on a cell suspension of 1 mL with $1x10^8$ cells, however the appropriate volume was calculated for each sample depending on the number of $CD4^+$ T cells in the suspension. For cell numbers that were under $1x10^7$, suspension volume was at 100 µL.

The 1 mL of cell suspension in a 14 mL polystyrene tube, was mixed with Anti-Human CD32 (Fc gamma RII) Blocker at a concentration of 100 µL/mL and 3.8 µL/mL of the CD45RO-PE antibody and incubated for 15 minutes at RT. 10 mL of isolation buffer was added, and the mixture was centrifuged at 340g for 10 minutes at RT. Supernatant was removed and the cells were resuspended in 1 mL isolation buffer. 100 µL of EasySep™ PE Selection Cocktail was added, and the mixture was incubated for 15 minutes at RT. EasySep™ Dextran RapidSpheres™ were vortexed for 30 seconds and 50 µL was added to the mixture, then incubated for 10 minutes at RT. To wash cell sample, isolation buffer was added to the mixture to reach a total of 2.5 mL and the mixture was placed on a magnet for 10 minutes at RT. The supernatant with the naïve cells were poured into a new tube. Wash step was repeated four times for half of the experiments, due to lower purity observed in flow analysis.

3.5.3 Harvesting $CD4^+$ naïve T cells

$CD4^+$ naïve T cells were centrifuged at 340g for 10 minutes at RT and the supernatant was removed. The cells were resuspended in 500 µL of isolation buffer and transferred to sterile 1.5 mL Eppendorf tubes. Cell suspension was centrifuged once more at 340g for 10 minutes, and the supernatant was carefully removed using a pipette, leaving a dry pellet of cells. The cells were immediately stored in a freezer at -80°C.

3.6 RNA extraction from $CD4^+$ naïve T cells

The RNA of $CD4^+$ naïve T cells was isolated using the RNA/DNA/Protein Purification Plus Kit (Norgen Biotek Corp., Canada). The RNA extraction was performed in a benchtop fume hood and equipment was wiped with RNase Away™ Decontamination Reagent (Thermo Fisher Scientific) prior to extraction.

Lysis Buffer Q was prepared for all samples, in total 8 (+ 1) samples per experiment. 300 µL of buffer was needed for each sample giving a total of 2.7 mL of buffer. 10 µL of β-mercaptoethanol was added to each 1 mL of buffer, giving a total of 27 µL of β-mercaptoethanol added to the buffer. Cells were taken directly out of -80°C freezer and put on dry ice. 300 µL of the Lysis Buffer Q was added to the frozen cell pellet, and the cells were lysed by vortexing for 15 seconds. The lysate was spun down quickly and passed through a 21-gauge needle attached to a 1 mL syringe five times to dissolve the cell pellet completely. Up to 600 µL of the lysate was added to a gDNA Purification Column pre-assembled in a collection tube and centrifuged at 5800g for 1 minute. The flowthrough of the lysate contained the RNA and proteins while the column contained the gDNA.

For every 100 µL of the flowthrough, 60 µL of 96 % EtOH was added to the collection tube and the mixture was resuspended with a pipette 10 times. Up to 600 µL of the mixture was added to an RNA purification Column pre-assembled in a collection tube and centrifuged at 3500g for 2 minutes. 400 µL of Wash Solution A was added to each column and samples were centrifuged at 14000g for 2 minutes. A mix of 15 µL DNase I and 100 µL Enzyme Incubation Buffer was made for each sample, and 100 µL of the buffer was added to each column and centrifuged at 14000g for 1 minute. Flowthrough was pipetted back into the column and incubated for 15 minutes. 400 µL of wash solution A was added to each column and centrifuged at 3500g for 1 minute. The flowthrough was discarded, and a second wash was done, followed by a centrifugation at 14000g for 2 minutes. Columns were placed in Elution tubes and 50 µL of Elution Solution A was added to each column and incubated at RT for 2 minutes. Samples were centrifuged at 200g for 1 minute followed by 5800g for 2 minutes and 14000g for 30 seconds. 45 µL of the samples were stored in -80°C freezer for future cDNA synthesis and the remaining 5 µL were used for quality control of the RNA.

3.6.1 RNA quality control and concentration measurement

Quality control of the extracted RNA was carried out using the 2100 Bioanalyzer Instrument (Agilent Technologies, USA) and RNA 6000 Nano Kit (Agilent Technologies). The Bioanalyzer Instrument was washed once with 350 μL of RNase Away^{TM} Decontamination Reagent and three times with 350 μL of Nuclease-Free Water prior to the run. RNA dye concentrate was placed at RT for 30 minutes and then 1 μL of the dye was added into a premade 65 μL filtered gel. The gel-dye mixture was added onto the chip using a Chip Priming Station (Agilent Technologies). 5 μL of RNA marker and 1 μL of $CD4^+$ T cell samples was added to all 12 sample wells. 5 μL of RNA marker and 1 μL of ladder was added to the ladder well. The chip was vortexed for 1 minute at 2400rpm and placed in the Bioanalyzer instrument for analysis, within 5 minutes after vortexing. The RNA integrity number (RIN) and the total amount of RNA in each sample was determined using the 2100 Bioanalyzer Expert Software (Agilent Technologies).

3.7 Statistics

Statistics were calculated using either GraphPad Prism 9 or Microsoft Excel v. 16.60. All error bars in this thesis are standard error of the mean (SEM), unless stated otherwise.

4 Results

4.1 Establishment of an optimized cell culturing protocol

The $CD4^+$ naïve T cell cultivation process was optimized by the selection of an appropriate activator and examination of culture morphology, viability, and purity. An optimized culture timeframe was also established for the best possible isolation of healthy, $CD4^+$ naïve T cells. In order to carry out the optimization, cells were isolated from six buffy coats from six different healthy individuals in separate experiments.

4.1.1 $CD4^+$ naïve T cells have a higher viability over time when incubated with CD3/CD28 T cell activator compared to CD3/CD28/CD2 T cell activator

To optimize the cultivation of $CD4^+$ naïve T cells, the activator used for further experiments was determined. Two activators were tested, CD3/CD28 T cell activator and CD3/CD28/CD2 T cell activator. After $CD4^+$ naïve T cells were isolated from the buffy coat on day 0, the cell suspension was divided into two flasks, where each flask was treated with a different activator. Viability and morphology of the cells were examined on day 3 and day 5, where the cells were inspected under the microscope. The cells treated with the CD3/CD28 activator were observed to have a higher density than the cells treated with the CD3/CD28/CD2 activator (not shown). This was confirmed when using the Nucleocounter®, where the cells treated with the CD3/CD28 activator had a higher cell count of $8.2x10^5$ cells/mL and a higher viability of 98.2% on day 3, in comparison with cells treated with the CD3/CD28/CD2 activator that had a cell count of $7.9x10^5$ cells/mL with a 95.9% viability (Figure 4.1). On day 5 the cells treated with the CD3/CD28 activator had a significantly higher viability ($p < 0.001$, ***) compared to the CD3/CD28/CD2 activator (Figure 4.1). The CD3/CD28 activator had a cell count of $4.2x10^5$ cells/mL and a 97.4% viability, while the cells treated with the CD3/CD28/CD2 activator had a cell count of $2.2x10^5$ cells/mL and a 90.8% viability. The CD3/CD28 T cell activator was therefore selected for use in all further cultivation of $CD4^+$ T cells.

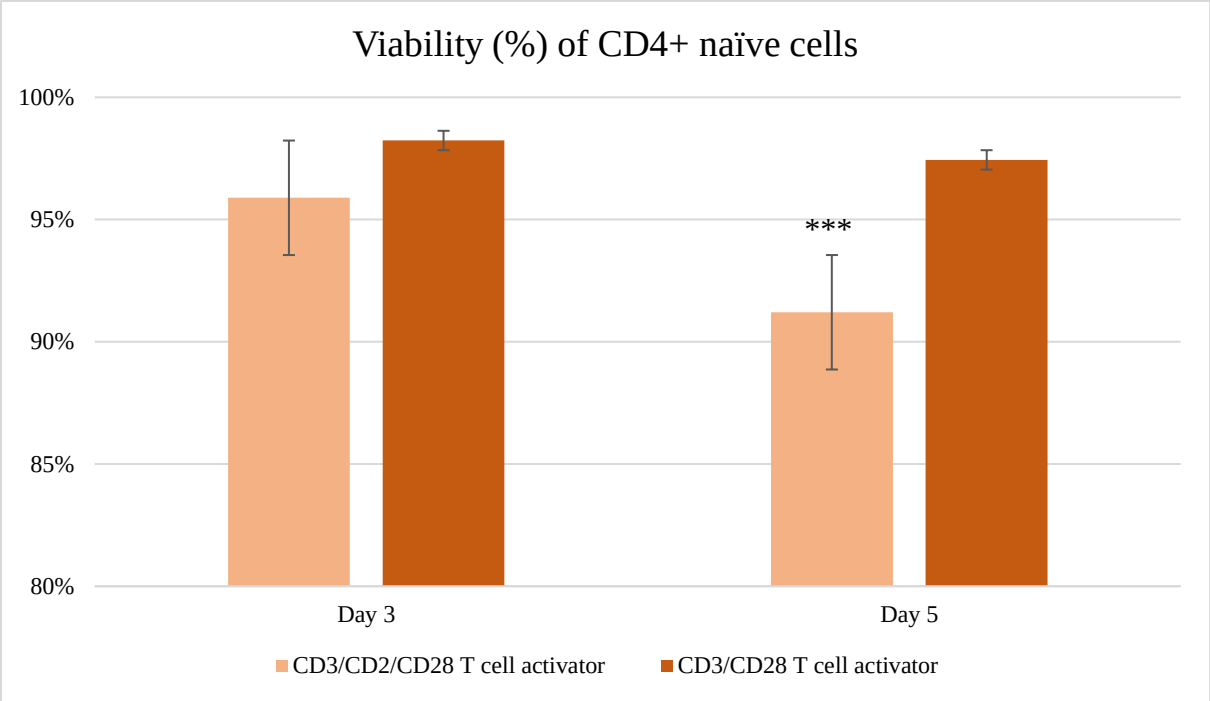

Figure 4.1: Cell viability after incubation with activators. Viability of the $CD4^+$ naïve T cells cultivated with either of two activators, CD3/CD28/CD2 T cell activator or CD3/CD28 T cell activator, were calculated using total- and non-viable cell counts from day 3 and day 5 of cell cultivation. Viability is shown as a percentage with graph starting at 80% viability. Samples were counted in triplicate, statistics: T-test, $p < 0.001$. Statistical analysis was not performed for results on day 3, as the CD3/CD28/CD2 T cell activator samples were only repeated twice.

4.1.2 Morphology of the $CD4^+$ naïve T cell population changed over time

The $CD4^+$ naïve T cells were observed by microscopy every day during the cell cultivation process to assess possible (i) morphology of cells, (ii) cell growth, (iii) density, and (iv) contamination. Upon examination, it was observed that the cells increasingly aggregated with time (Figure 4.2). Cells were seeded out in a homogenous cell suspension on day 0. On day 1 the cells had somewhat started to aggregate, however the majority of the cell population remained in their single cell state (Figure 4.2A). By day 2, more cells had aggregated into bigger clusters of cells and less cells were separated from these clusters (Figure 4.2B). Therefore, the cell suspension was carefully resuspended by pipetting up and down 10-20 times, to make the suspension as homogenous as possible before counting or further seeding out cells (Figure 4.3). It was also observed that the cells tended to sediment to the bottom of the cell culture flasks and plates over time. The additional resuspension also supported to loosen the cells from the plastic to promote a homogenous suspension.

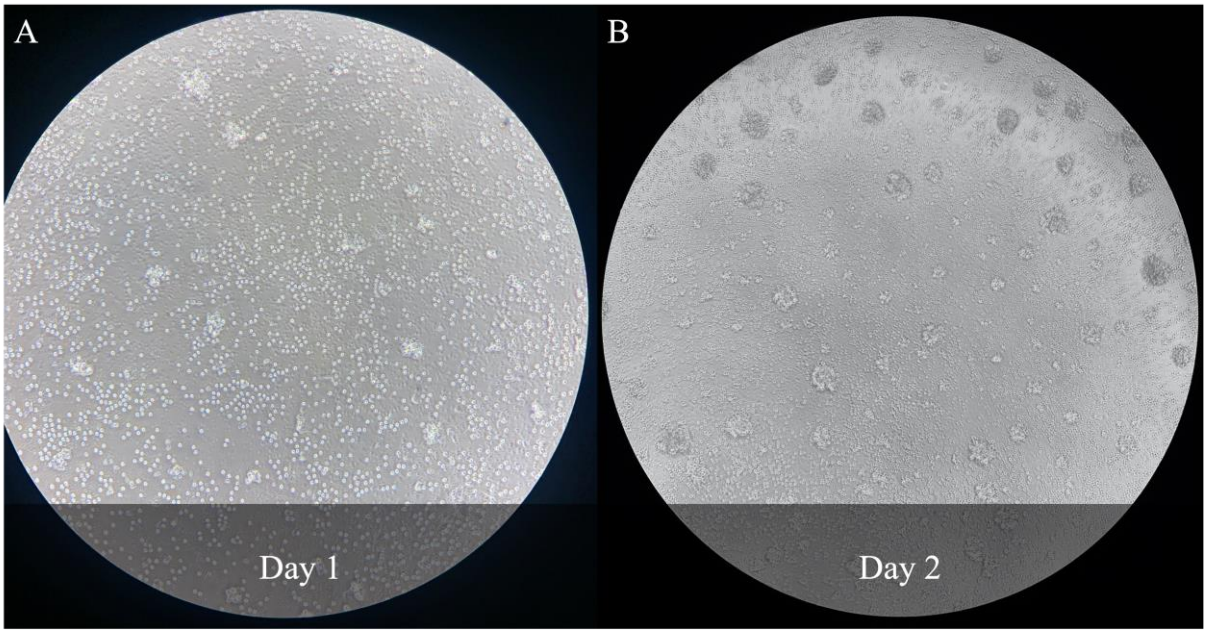

Figure 4.2: Microscopy images of aggregating cells. The $CD4^+$ naïve T cell culture examined at 10x magnification on day 1 (A) and day 2 (B) of the cell cultivation process. More aggregated cell clusters were observed at day 2 compared to day 1. The images were from the same cell sample.

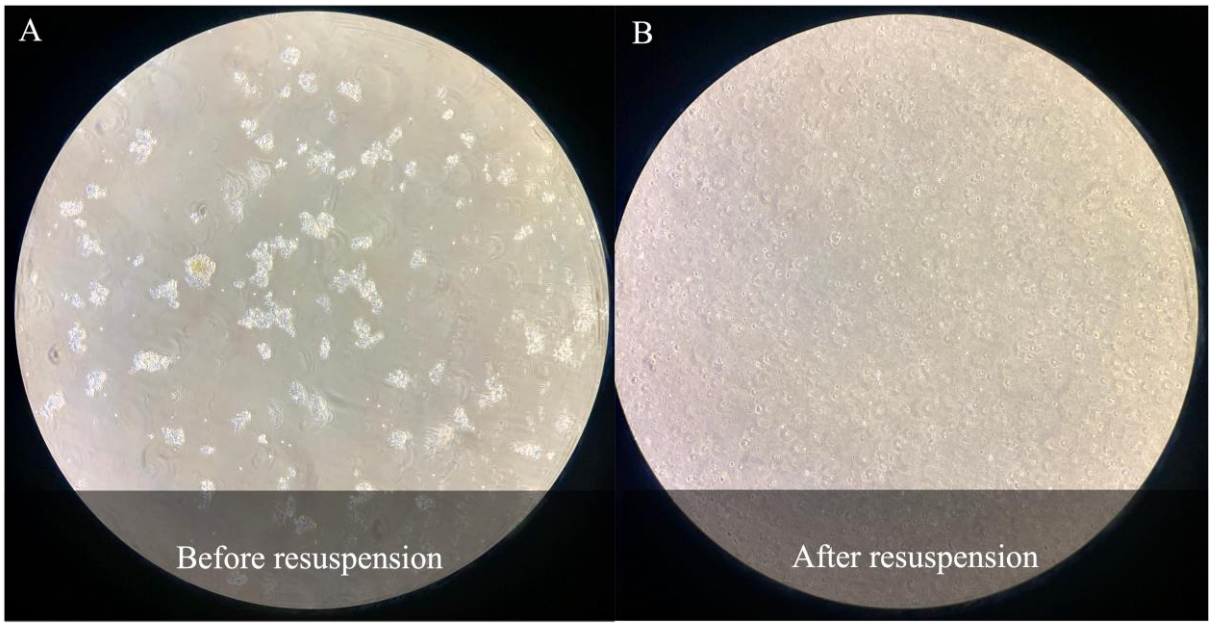

Figure 4.3: Microscopy images of cells prior to- and after resuspension. The $CD4^+$ naïve T cell culture was observed at 10x magnification before and after resuspension of the cells. Less cells were aggregated into clusters after resuspension, compared to before resuspension. The images were taken on the same cell sample on day 2 of cell cultivation, before (A) and after (B) the resuspension procedure.

4.1.3 Viability of CD4$^+$ naïve T cells gradually decreased over time

The initial cell cultivation protocol involved culturing CD4$^+$ naïve T cells over 7 days, where the naïve cell population was isolated on day 0 and cultured to day 7. To achieve the optimal viable cell density, the cell suspension was diluted 8-folds on day 3 and 4-folds on day 5. The cells were counted throughout the cell cultivation process, and viability was calculated as in Section 4.1.1. Although the viability of the CD4$^+$ naïve T cells was still reasonably high on the day 7 of cultivation, it did decrease gradually from day 0 with a viability of 99.6% to a viability of 93% on day 7 (Figure 4.4).

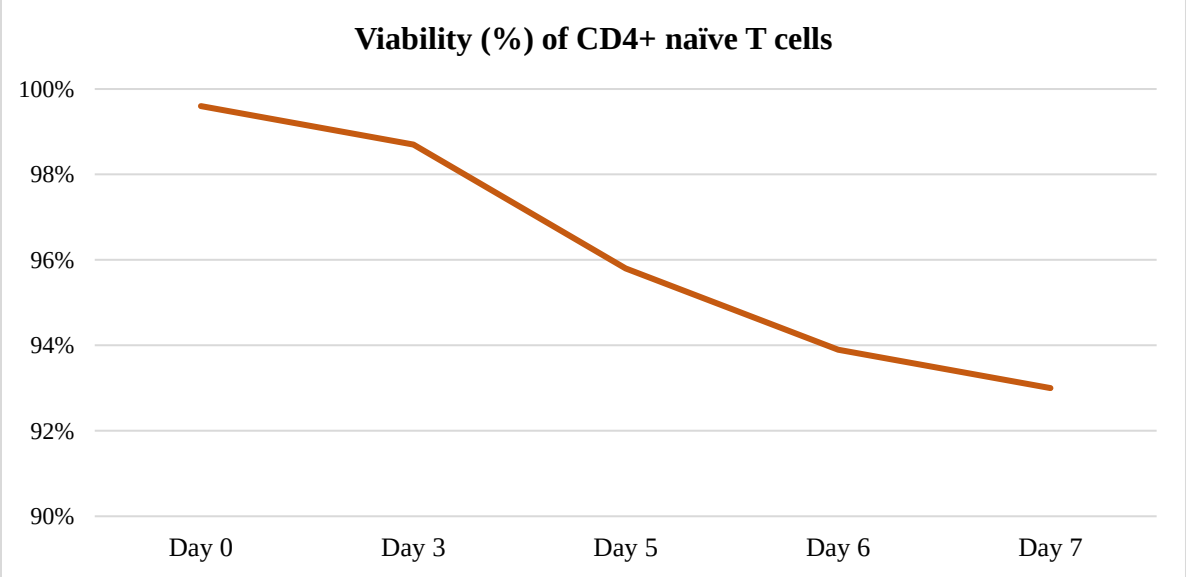

Figure 4.4: Cell viability of CD4$^+$ naïve T cells during cultivation. CD4$^+$ naïve T cells were counted from day 0 to day 7 of cultivation, where day 0 represents the day that the naïve cells were isolated and the initial start of cell cultivation and day 7 represents the final day. Viability (%) of the cells was calculated manually from the total cell counts and non-viable cell counts obtained from the NucleoCounter®. Viability is shown as a percentage with graph starting at 90% viability.

4.1.4 Apoptosis, and purity of cell samples in regard to CD8, CD3 and CD68.

Apoptosis and the purity of the CD4$^+$ naïve T cells samples was investigated regularly by flow cytometry during the cell cultivation process. AnnexinV was used as a stain to detect early apoptosis in the CD4$^+$ T cells. However, all samples had a high apoptotic ratio for the majority of cells in each sample, an example of this is shown in Figure 4.5A. Due to the unusually high apoptotic rate determined by AnnexinV, the NucleoCounter® was used to assess viability for all future experiments, which reported much lower and expected cell death (< 10% dead cells). The purity of the samples was also examined using flow cytometry. Results from the analysis

showed no $CD8^+$ T cells in the samples (Figure 4.5A), however there were $CD3^+$ cells present in most of the cell populations (Figure 4.5B). CD68 was used as a surface marker for monocytes, however no monocytes were present in the sample (Figure 4B).

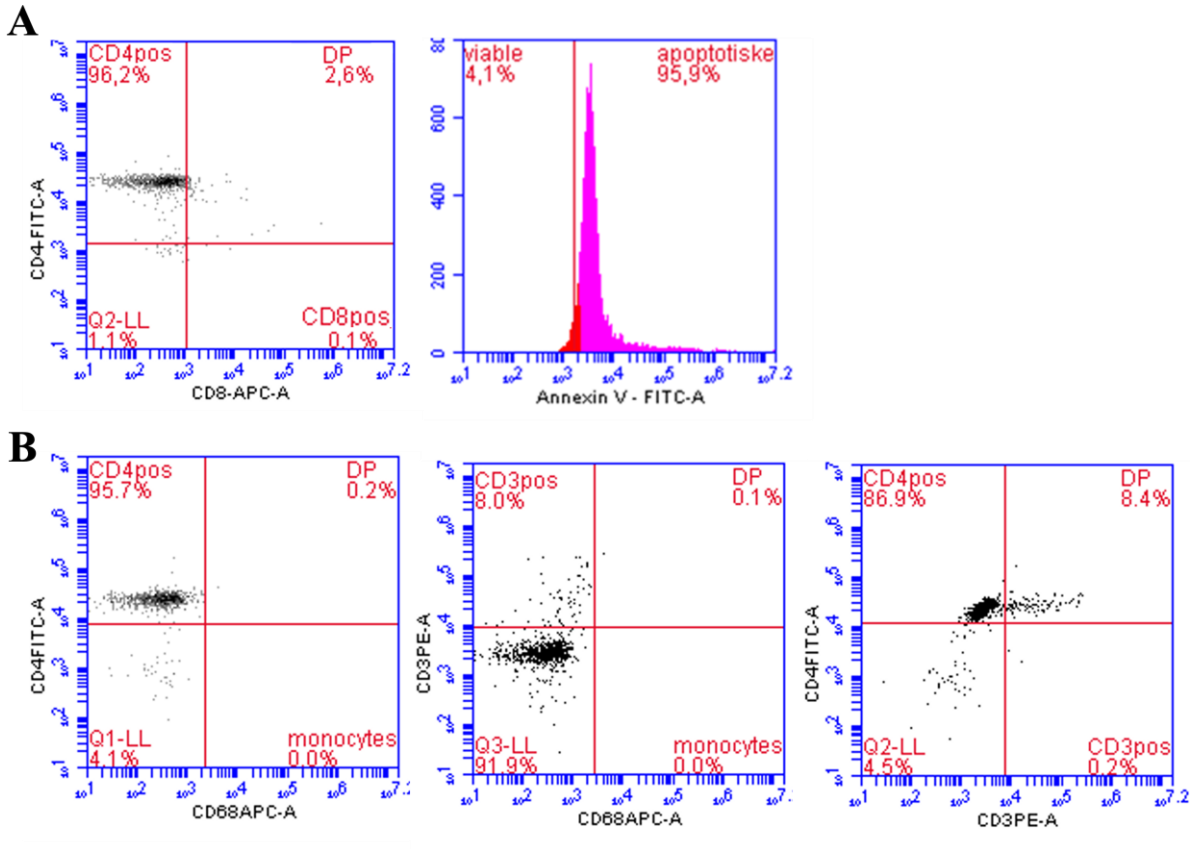

Figure 4.5: Purity, apoptosis and possible monocytes in $CD4^+$ T cell samples. A selection of data from purity and apoptotic analysis of the untreated $CD4^+$ T samples were examined with markers for CD8, CD3 and CD4 in order to look at the ratio of the cells. (A) The ratio of CD4 to CD8 in one sample, with the corresponding apoptotic marker for the same sample. (B) The ratio of CD4 to CD3 to CD68, where CD68 was used as a surface marker for monocytes. DP = Double positive.

4.1.5 Naïve $CD4^+$ T cells converted to memory cells with time

The $CD4^+$ naïve T cell population was analyzed using flow cytometry to examine the purity of the isolated naïve cell population. As the isolation method is not expected to give a 100% pure naïve ($CD45RA^+CD45RO^-$) cell population, flow cytometry was used to assess how many memory ($CD45RA^-CD45RO^+$) cells had remained after the isolation process. Surprisingly, even though the $CD4^+$ T cells had been isolated into the naïve ($CD45RA^+CD45RO^-$) subgroup on day 0, the naïve cell population only accounted for 13.8% of the total cell population by day 6 (Figure 4.6A). While some memory ($CD45RA^-CD45RO^+$) cells were present (9.3%), the majority of the day 6 cells were double positive ($CD45RA^+CD45RO^+$) cells adding up to 75.7%

of the total cell population. This could indicate that the naïve cell population was converting to memory cells over time, through a double positive, memory-like cell state. To confirm if the naïve T cell population decreases over time, and to determine the change in the naïve to memory cells ratio during the cell cultivation process, a new analysis by flow cytometry was performed on day 2 and day 5 of the cell cultivation process in a new buffy coat, which also includes an initial analysis performed immediately after isolation on day 0. The data from this analysis showed a dramatic decrease in the naïve T cell population from 83% on day 2 and even further 17.0% on day 5 (Figure 4.6B), after a much more subtle decrease from 87% to 85% between day 0 and day 2 respectively. Thus, indicating that the majority of the naïve $CD4^+$ T cell population developed into memory cells between days 3 and day 5 during the T cell cultivation protocol. While it is clear the naïve $CD4^+$ T cells convert to memory cells between days 3 and 5, two distinct populations representing naïve and DP cells can be seen are much clearer on day 4 than in Figure 4.6 (Appendix III).

4.1.6 Isolating naïve subgroup as last step of cell protocol

As the previous analysis revealed that the majority of the initially isolated $CD4^+$ naïve T cells remained naïve until day 2, the protocol was shortened to only 2 days. Using a new buffy coat, the memory and naïve ratio was once again examined on day 0 and day 2 for comparison. On day 0, the population of naïve cells was 81.2% after the isolation of the naïve cell population, and on day 2 the population had decreased to 73.5% (Figure 4.6C). In the experiments presented here and above, the $CD4^+$ T cells had been isolated into a naïve subgroup on day 0. The reason to isolate the $CD4^+$ T cells into a naïve subgroup on day 0 was to ensure a purest naïve cell population as possible. However, due to the observation that $CD4^+$ naïve T cells were gaining the memory phenotype and converting into memory cells over time, it was decided to isolate the $CD4^+$ naïve cells on the last day of cell cultivation, rather than on the first day, for all further experiments. Therefore, all the later stimulation experiments were performed on the total $CD4^+$ T cell population instead of specifically on isolated $CD4^+$ naïve T cells. Upon T cell cultivation and treatment of the total cell population on day 0, the $CD4^+$ naïve T cell population was isolated upon assay/cultivation completion, harvested and frozen for further analysis.

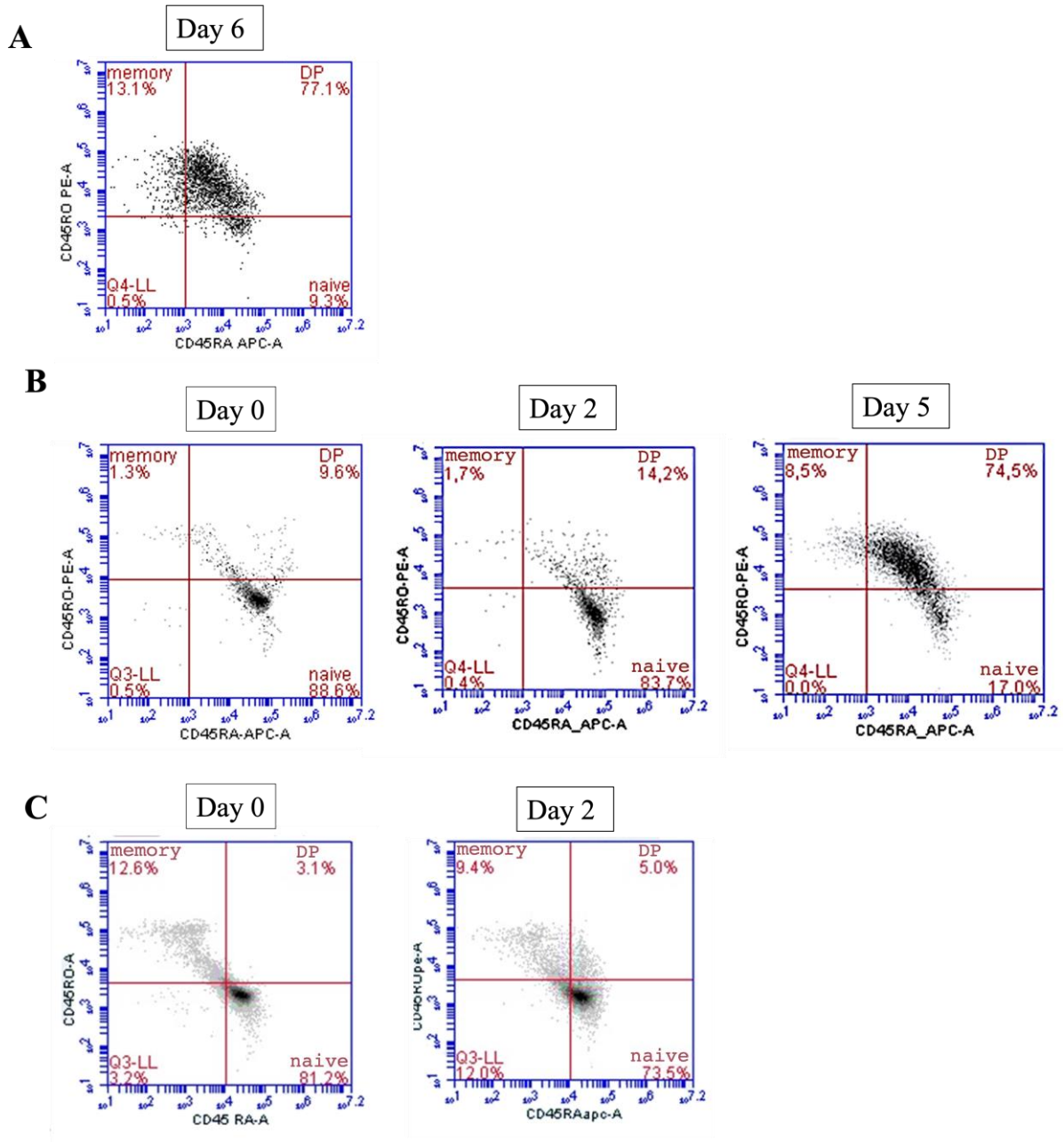

Figure 4.6: Ratio of naïve to memory T cells. The naïve to ratio purity of $CD4^+$ naïve T cells ($CD45RA^+$) was analyzed after various days of cultivation, using the BD Accuri C6 flow cytometer to examine the ratio of $CD45RO^+$ and $CD45RA^+$ cells in the sample. CD45RA was used as a surface marker for naïve cells and CD45RO as surface marker for memory cells. (A) to (C) represent flow cytometry results from three independent buffy coats. (A) The naïve and memory T cell ratio on day 6. (B) The naïve and memory cell ratio on day 0, day 2 and day 5. (C) The naïve and memory cell ratio of cells on day 0 and day 2. For (B) and (C), the naïve $CD45RA^+CD45RO^-$ cells are in the bottom right corner, the memory $CD45RA^-CD45RO^+$ cells are in the top left corner, and the double positive (DP) $CD45RA^+CD45RO^+$ are in the top right corner.

4.2 WST-1 assay was used to determine the concentrations of MTX and nicotine for treatment of $CD4^+$ T cells

To determine the appropriate concentrations of MTX and nicotine to stimulate the $CD4^+$ T cells, a WST-1 cell proliferation assay was performed.

4.2.1 Optimize plate set-up to reduce background

While performing the initial WST-1 assay, it was observed that high variability of the background control wells led to variability within the result data. Therefore, the plate layout had to be optimized in order to include additional replicates to decrease background noise in the data and increase accuracy. $CD4^+$ T cells were incubated with different concentrations of MTX and nicotine in 96-well plates, 24/48 hours respectively, prior to the WST-1 assay. The initial plate set-ups included four replicates for each of the eight concentrations tested for MTX and four concentrations tested for nicotine. Additionally, duplicates without cells were added for each concentration to remove background noise resulting from the media or the treatments, for each sample (Figure 4.7). While the background wells theoretically should have been approximately the same across all wells, high variability in the absorbance data within the duplicate background wells (and some of the sample wells) was observed (not shown). As such, more replicates for the background were needed in further experiments, to counteract this variability, however there was also a consideration of space in the 96-well plate. Another refined layout of the plates was made with more replicates of the MTX and nicotine concentrations as well as more replicates for the background (Figure 4.8). For the background wells without cells, both samples with the highest concentration of MTX or nicotine were included and compared to samples without the treatment. This was done to ensure that the addition of MTX or nicotine did not affect the absorbance read. This successfully reduced variability from background noise, and the plate set-up was used for all further WST-1 experiments (Figure 4.8).

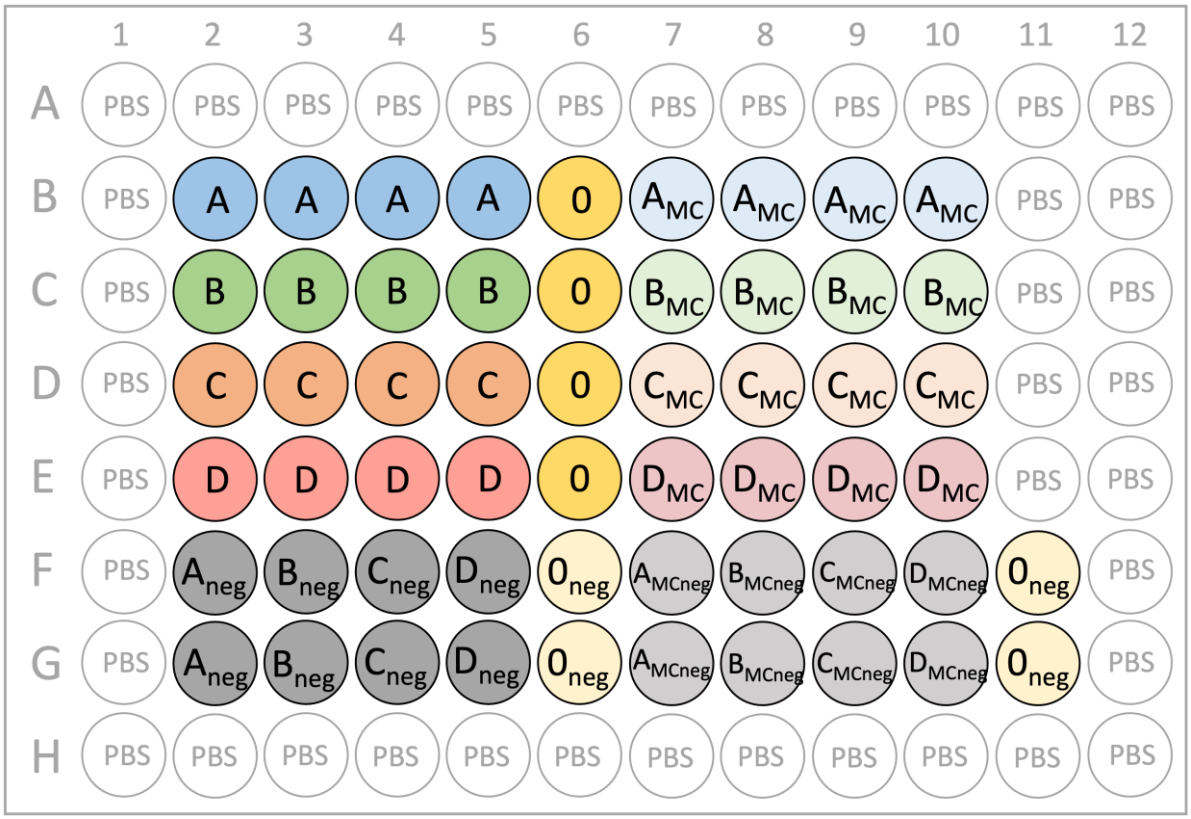

Figure 4.7: Initial experimental 96-well plate setup for the WST-1 assay. $CD4^+$ T cells were treated with various concentrations of MTX or nicotine in each 96-well plate. In total, eight concentrations of MTX were tested in two separate plates, and four concentrations of nicotine were tested in a single plate. The initial plate setup included a total of four replicates of each concentration, and duplicates for the background control of treatment samples and four replicates for the untreated samples.

A, B, C & D = cell samples with different concentration of MTX or nicotine.

0 = positive control (untreated cell samples).

A_{neg}, B_{neg}, C_{neg}, D_{neg} & 0_{neg} = negative controls (media + treatment – cells).

A_{MC}, B_{MC}, C_{MC} & D_{MC} = mock controls for each concentration (media + mock treatment + cells).

A_{MCneg}, B_{MCneg}, C_{MCneg} & D_{MCneg} = negative controls for mock controls (media + mock treatment – cells).

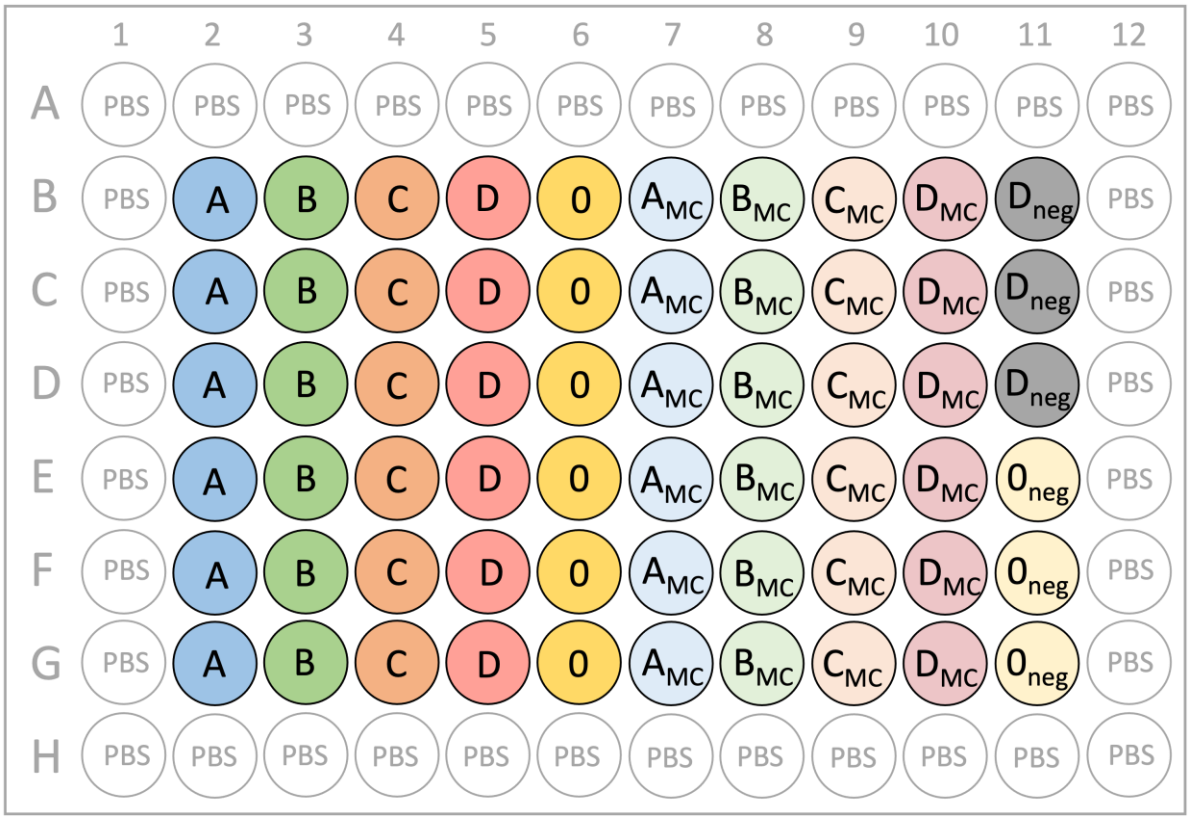

Figure 4.8: Final experimental 96-well plate setup for the WST-1 assay. $CD4^+$ T cells were treated with various concentrations of MTX or nicotine in each 96-well plate. In total eight concentrations of MTX were tested in two separate plates, and four concentrations of nicotine were tested in a single plate. The final plate setup included a total of six replicates of each concentration and 2x3 replicates for the background control, three with the highest treatment concentration and three untreated.

A, B, C & D = cell samples with different concentration of MTX or nicotine.

0 = positive control (untreated cell samples).

A_{neg}, B_{neg}, C_{neg}, D_{neg} & 0_{neg} = negative controls (media + treatment – cells).

A_{MC}, B_{MC}, C_{MC} & D_{MC} = mock controls for each concentration (media + mock treatment + cells).

4.2.2 Determining the appropriate incubation time with the cell proliferation agent WST-1

To analyze cell viability, the WST-1 reagent is incubated with cells over an optimized time, to establish the best resolution for measuring relative cell proliferation. To determine the appropriate incubation time of treated $CD4^+$ T cells with the WST-1 reagent, multiple incubation timepoints were tested. For the first experiment, the 96 well plate was incubated for up to 90 minutes with WST-1. However, it was observed that the relative cell proliferation across the tested MTX concentrations varied more for the 30-minute incubation than for the 60- and 90-minute incubation (Figure 4.9A). The same trend was observed in the relative

proliferation of cells treated with nicotine (Figure 4.9B), thus the timepoint was excluded for further assays. To determine whether the proliferation would be influenced by longer incubation time with WST-1, additional timepoints up to 240 minutes were included, as supported by the Sigma-Aldrich Protocol Guide: WST-1 Assay for Cell Proliferation and Viability (61). However, the proliferation seemed to stabilize at for all tested MTX and nicotine concentrations after 90 minutes of incubation (Figure 4.10A&B). It was also noted that there was no observed change in relative proliferation of $CD4^+$ T cells upon treatment with MTX or exposure with nicotine after 24 or 48 hours respectively, at all concentrations tested.

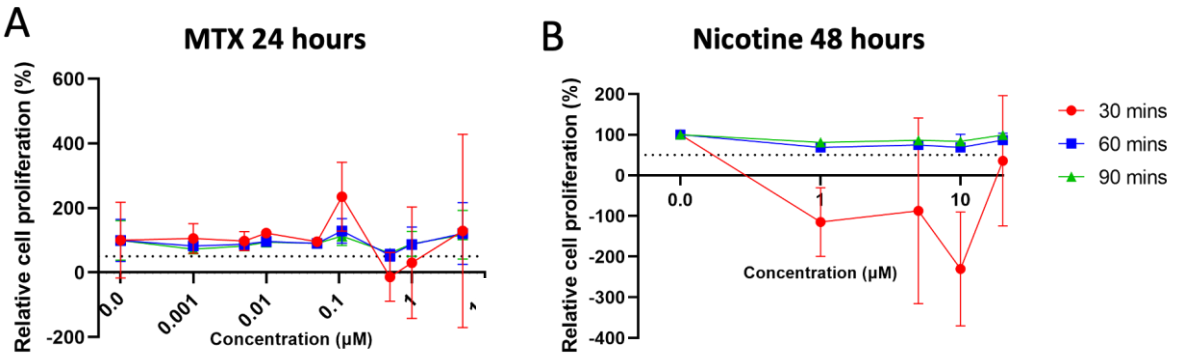

Figure 4.9: WST-1 activity at timepoints up to 90 minutes. $CD4^+$ T cells were incubated with (A) MTX and (B) nicotine for 24 hours and 48 hours, respectively. WST-1 cell proliferation agent was added to each sample and absorbance was read at 30- 60- and 90 minutes. The y-axis show the percentage of relative cell proliferation in relation to the concentration (μM) of MTX or nicotine represented in the x-axis. Data is presented as the mean ± SE of every concentration performed in four replicates.

4.2.3 Determining incubation time with MTX

To determine the appropriate incubation time and concentrations of MTX for treatment of $CD4^+$ T cells, the WST-1 assay was repeated for cells treated with MTX at 24 and 48 hours. Multiple WST-1 incubation times were included, from 60 to 240 minutes. The cell proliferation measured after 24 hours of incubation with increasing concentrations of MTX did not seem to affect the relative cell proliferation (Figure 4.10A), concurring with previous observations (Figure 4.9A). However, at 48 hours, increasing MTX concentration did lead to a decrease in cell proliferation when the MTX concentration was >0.005 μM (Figure 4.10B). The same trend was observed in an additional assay where another buffy coat was used (Figure 4.10C&D). MTX mock samples were also performed (see Appendix IV).

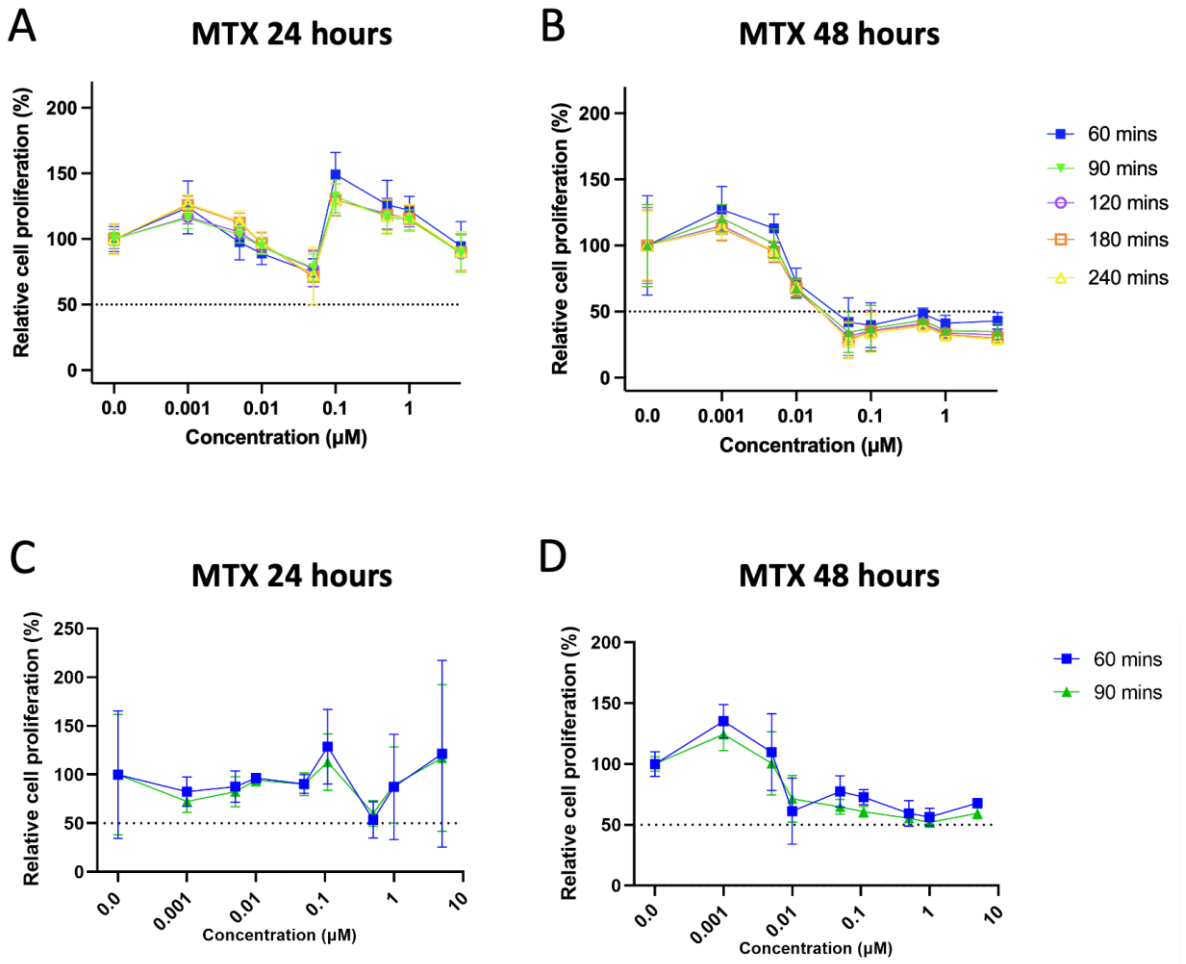

Figure 4.10: Effects of MTX on relative cell proliferation of CD4⁺ T cells. Cells were treated with concentrations of MTX ranging from 0.001 µM to 5 µM. Relative cell proliferation was measured after 24 and 48 hours of incubation, using the WST-1 assay. The plates were incubated with WST-1 and absorbance was determined at timepoints ranging from 60-240 minutes. (A) Relative cell proliferation of cells incubated with MTX for 24 hours, including incubation with WST-1 up to 240 minutes for the first buffy coat. (B) Relative cell proliferation of cells incubated with MTX for 48 hours, including incubation with WST-1 up to 240 minutes for the first buffy coat. (C) Relative cell proliferation of cells incubated with MTX for 24 hours and incubation with WST-1 up to 90 minutes for the second buffy coat. (D) Relative cell proliferation of cells incubated with MTX for 48 hours and incubation with WST-1 up to 90 minutes for the second buffy coat. The y-axis shows percentage of relative cell proliferation in relation to the concentration (µM) of MTX represented in the x-axis. Data is presented as the mean ± SE of every concentration performed in six (A & B) and four (C & D) replicates.

4.2.4 Determining optimal exposure concentration of nicotine for CD4$^+$ T cells

The intention behind trying to find a suitable nicotine concentration was to find one that did not change the relative cell proliferation of the CD4$^+$ T cells. The results from the WST-1 assay, after 48-hour incubation with nicotine, showed that none of the nicotine concentrations tested had an effect on relative cell proliferation of the CD4$^+$ T cells (Figure 4.11A). Mocks with additional EtOH corresponding with the EtOH used to dilute the nicotine concentration, but without nicotine was also included (Figure 4.11B). This was done in order to assess whether the EtOH could be responsible for any changes in the relative cell proliferation of the CD4$^+$ T cells. The results suggest that EtOH did not affect the relative cell proliferation of the CD4$^+$ T cells. The concentration of 10 µM nicotine was therefore chosen for further experiments as the cell proliferation seemed unaffected by the concentration (Figure 4.12), and based on previous literature (63).

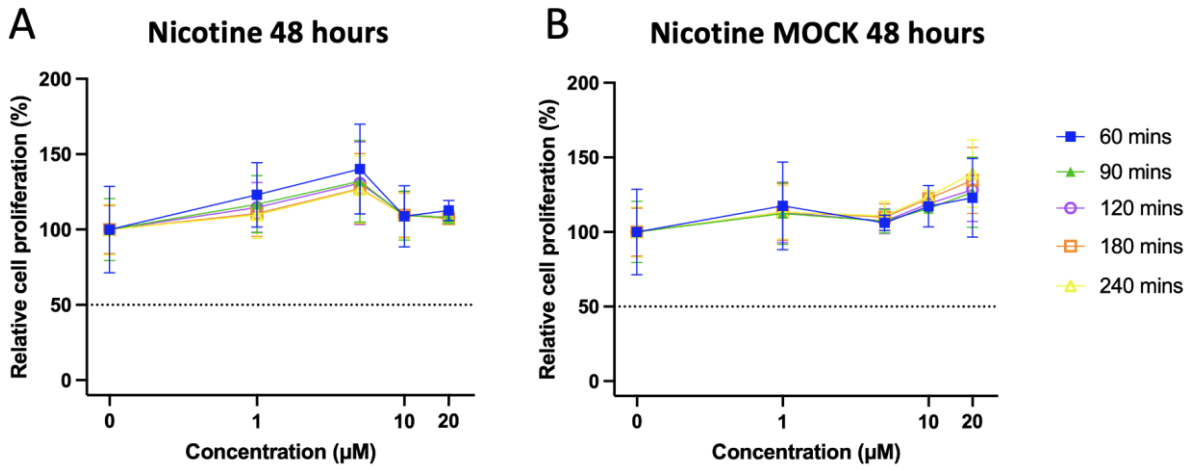

Figure 4.11: Effects of nicotine on relative cell proliferation of CD4$^+$ T cells. Cells were treated with concentrations of nicotine ranging from 1 µM to 20 µM, and EtOH mocks without nicotine. Relative cell proliferation was measured after 48 hours of incubation, using the WST-1 assay. The 96-well plate was incubated with WST-1 and absorbance read at timepoints ranging from 60-240 minutes. The y-axis show the percentage of relative cell proliferation in relation to the concentration (µM) of nicotine or nicotine mock controls represented in the x-axis. Data is presented as the mean ± SE of every concentration performed in six replicates.

4.2.5 Final concentration of and MTX for treatment of CD4$^+$ T cells

Based on the 48-hour incubation study with MTX, the final concentrations of MTX were determined for use in further experiments. The concentrations selected for MTX were 0.005 µM, 0.01 µM and 0.05 µM, due to their effect on relative cell proliferation of approximately 100%, 60% and 40% respectively (Figure 4.9B). Since an incubation time of

48 hours was decided for both MTX and nicotine, the effects of the combination of nicotine and MTX treatment on the $CD4^+$ T cells could also be explored. The lowest and highest concentrations of MTX tested was therefore combined with 10 µM of nicotine. The samples tested also included a nicotine mock control, as well as an untreated control sample, making a total of eight different sample treatments. These specific treatment concentrations (described in Figure 4.12) were selected for possible further analysis of the $CD4^+$ T cells in response to treatment.

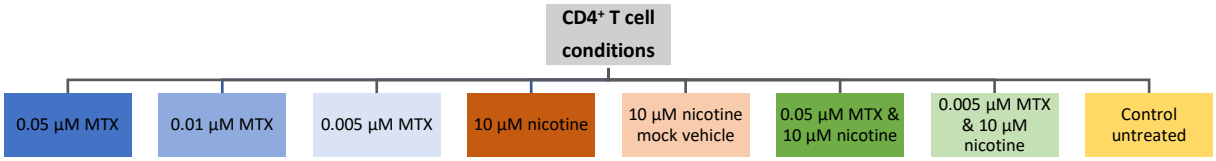

Figure 4.12: Overview of final $CD4^+$ T cell treatments. Cells were isolated from three healthy blood donors and treated with the different conditions described, before 48 hours of incubation and isolation of the naïve subtype.

4.3 Modification to washing frequency correlated with $CD4^+$ naïve T cell population capture

After the cell cultivation process had been optimized, this assay was used on another three new buffy coats from healthy donors (hereby Donor 1, 2 and 3). The $CD4^+$ T cells were isolated from the buffy coats and treated with the different conditions described (Figure 4.12). After the cells were incubated with their corresponding treatment conditions for 48 hours, the naïve subgroups were isolated, counted and characterized by flow cytometry as described in Section 4.1.6. The cell samples from Donor 1 were only washed once when isolating the naïve subgroup, but due to lower purity of naïve ($CD45RA^+CD45RO^-$) cells than expected after isolation (80.1% and 74.3% naïve T cell purity; Figure 4.14), three additional wash steps were included in the process for Donor 2. This was done both to ensure the purest sample possible of naïve T cells and to ensure that as many naïve cells as possible would be isolated from the sample. However, this resulted in less than half of the number naïve cells isolated compared to Donor 1 (Average 1.92 x 10^6 cells for Donor 1 compared to average 4.66 x 10^5 cells for Donor 2; Figure 4.13). To make sure that this was not due to more naïve T cells being present in the original total cell population at day 0, flow cytometry analysis was examined (Figure 4.14). At day 0, the 3 Donors had naïve T cell populations of 31.2%, 19.8%, and 13.8%

respectively. Therefore, for Donor 3, half of the 8 cell samples were washed four times while the other half were washed once, for comparison. Similarly to the results from Donor 1 and Donor 2, the cell samples from Donor 3 that were washed four times (MTX monotreatments and no treatment control) had about half of the naïve T cell population compared to the cell samples washed once (Nicotine, mock and MTX/nicotine combination treatments) (Figure 4.13).

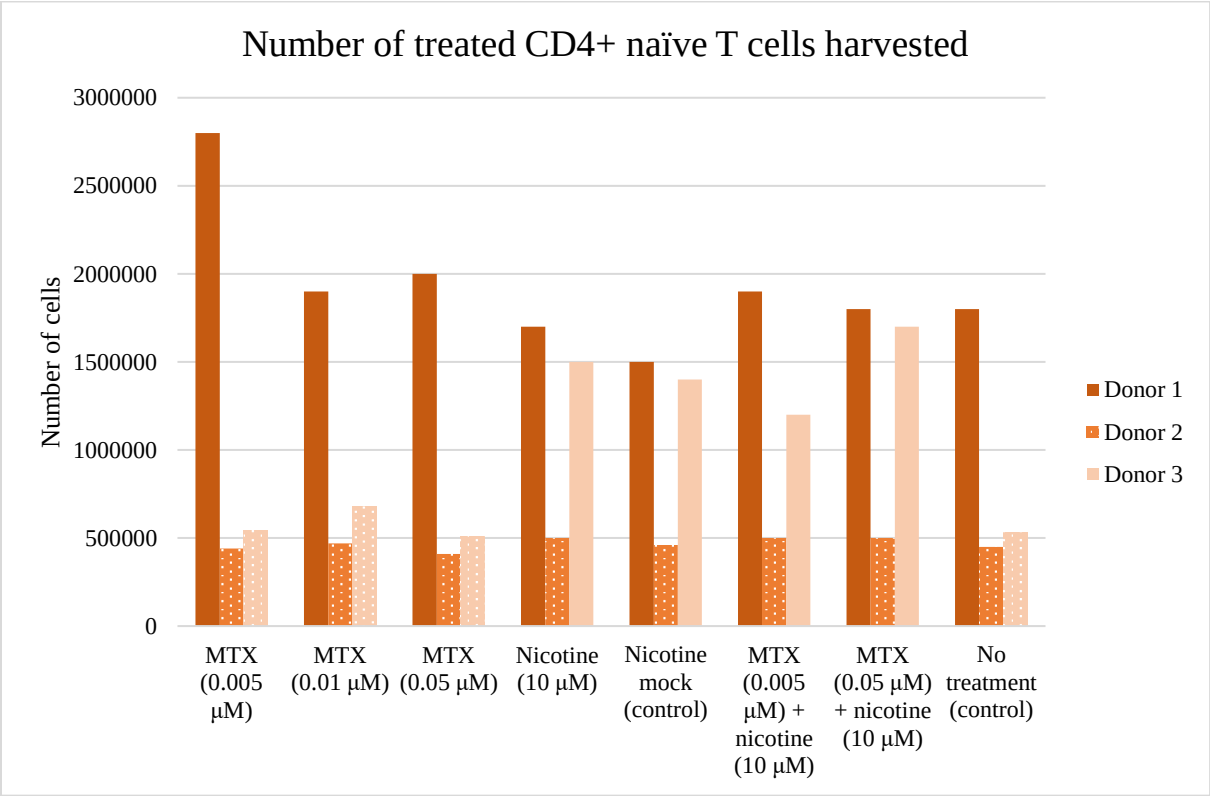

Figure 4.13: CD4$^+$ naïve T cell counts after 48-hour incubation with treatments and isolation of the naïve T cell population. Cells harvested from three different donors divided into 8 groups with different treatment conditions. The dotted bars are samples that were washed an additional three times, while the non-dotted bars were washed once. The nicotine mock (control) were cells treated with same concentration of EtOH as in the sample treated with nicotine (10 µM), but without the nicotine. Cell counts were performed using NucleoCounter® and Countess®.

The naïve to memory ratio was examined to discover if the extra washes, while reducing the total naïve cell number, improved overall naïve cell isolation purity. The naïve T cell population of the samples that had been washed additionally three times already appeared somewhat higher from Figure 4.14, so this analysis was expanded to include all flow analysis from all 3 Donors (Table 4.1). Looking at the average cell ratios from the isolated samples, it is clear that the cell

samples that were only washed once had a higher proportion of cells that were double positive ($CD45RA^+CD45RO^+$) and memory cells ($CD45RA^-CD45RO^+$), which could indicate that not all $CD45RO^+$ cells were properly washed away in a single wash step. This indicated that the counts of the $CD4^+$ naïve T cells from samples that were only washed once included more non-naïve cells (Figure 4.13), however this small discrepancy in purity doesn't explain the large difference seen between total T cell counts in the samples that are quadruple washed compared to washed once.

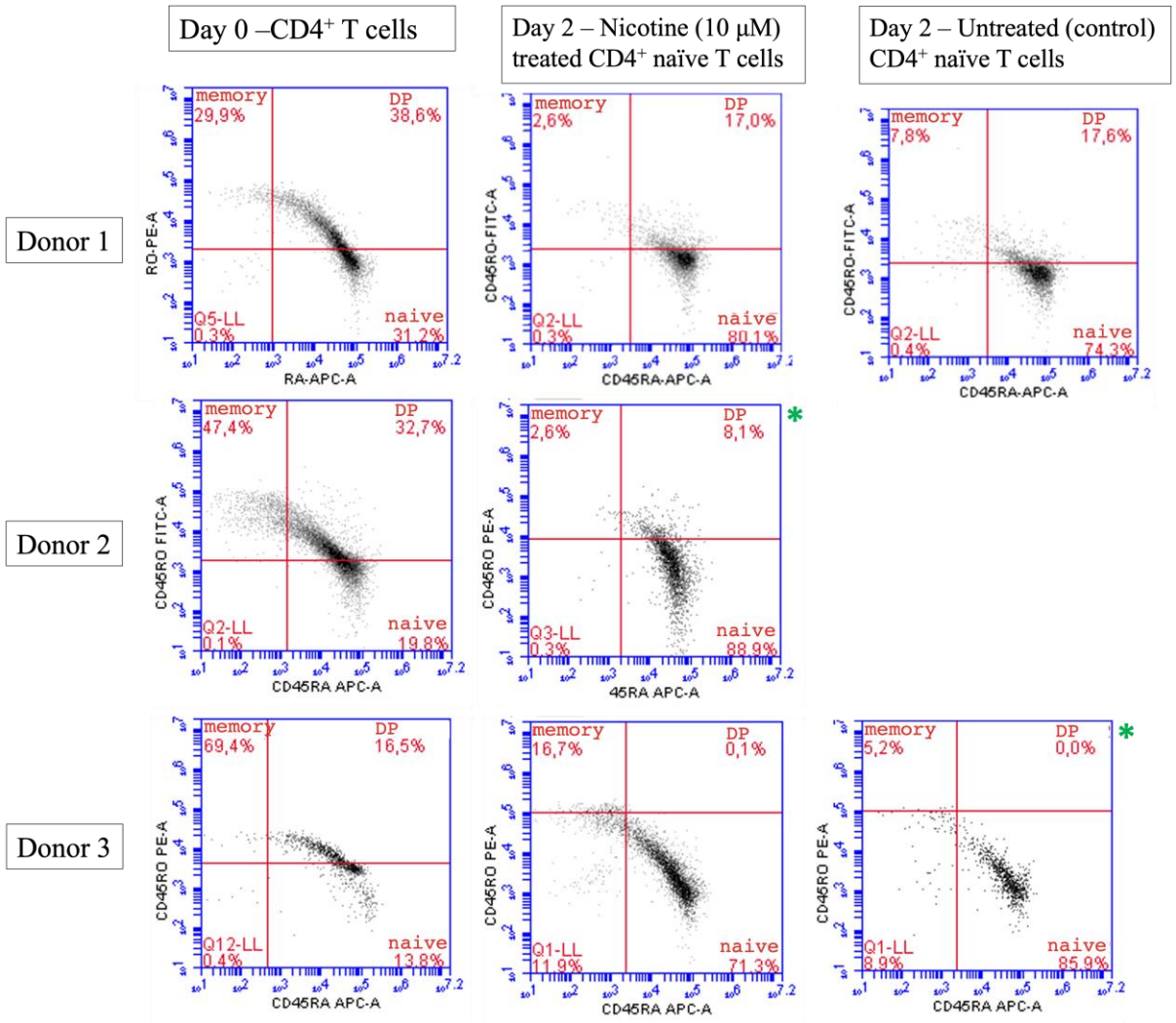

Figure 4.14: Ratio of memory and naïve subgroups for a selection of the $CD4^+$ T cell populations before (day 0) and after (day 2) isolation of naïve T cells. $CD4^+$ naïve T cells were run on the BD Accuri flow cytometer using CD45RA as surface marker for naïve cells and CD45RO as surface marker for memory cells. Day 0 shows the ratio of memory and naïve cells of total $CD4^+$ T cells. Day 2 shows the ratio of memory and naïve cells after isolation of the naïve T cell population, both for nicotine (10 µM) treated cells and untreated (control) cells. The untreated sample from day 2 donor two is missing due to the lack of cells. The flow charts marked with a star (*) are the samples that were washed an additional three times. DP = Double positive.

Table 4.1: Average ratio of naïve, memory and double positive CD4$^+$ T cells.

	Washed once	Washed 4 times
Naïve cells	74.7%	87.3%
Memory cells	9.3%	3.8%
Double Positive cells	12.6%	5.9%

Percentages taken from flow cytometry data (not shown).

4.4. RNA extraction from treated CD4$^+$ naïve T cells

RNA was extracted from isolated naïve CD4$^+$ T cells, in order to be establish if suitable RNA could be extracted using this cultivation method, for future genetic analysis. Total RNA was extracted from treated CD4$^+$ naïve T cells, and quality control of the extracted RNA was done using the 2100 Bioanalyzer. RNA integrity numbers (RIN) were obtained during quality control, which is a 1 (degraded) to 10 (intact) scale calculated by the quality of RNA separation in a sample. All samples had relatively large RIN values (≥ 9.1) (Table 4.2), which indicated that the integrity of the RNA did not seem to be affected by the additional wash of the samples or loss of cells. The amount of RNA that was harvested from each sample was approximately halved for the samples that had been additionally washed, confirming the previous cell count numbers where 50-70% of the cell material was gone (Figure 4.15).

Table 4.2: RIN values for all samples

Treatment	Donor 1*	Donor 2	Donor 3*
MTX (0.005 μM)	10.00**	9.60	9.10
MTX (0.01 μM)	9.80	9.60	9.40
MTX (0.05 μM)	9.30	10.00	9.50
Nicotine (10 μM)	10.00	9.70	9.50
Nicotine mock (control)	9.90	10.00	9.50
MTX (0.005 μM) + nicotine (10 μM)	10.00	9.50	10.00
MTX (0.05 μM) + nicotine (10 μM)	9.60	9.80	10.00
No treatment (control)	9.40	9.80	9.30
Average:	**9.75**	**9.75**	**9.54**
Average of samples with extra wash:			**9.61**
Average of samples washed once:			**9.75**

* Colored cells presented in the table are samples that were washed once.

** RIN ranges from 1 (degraded) to 10 (intact).

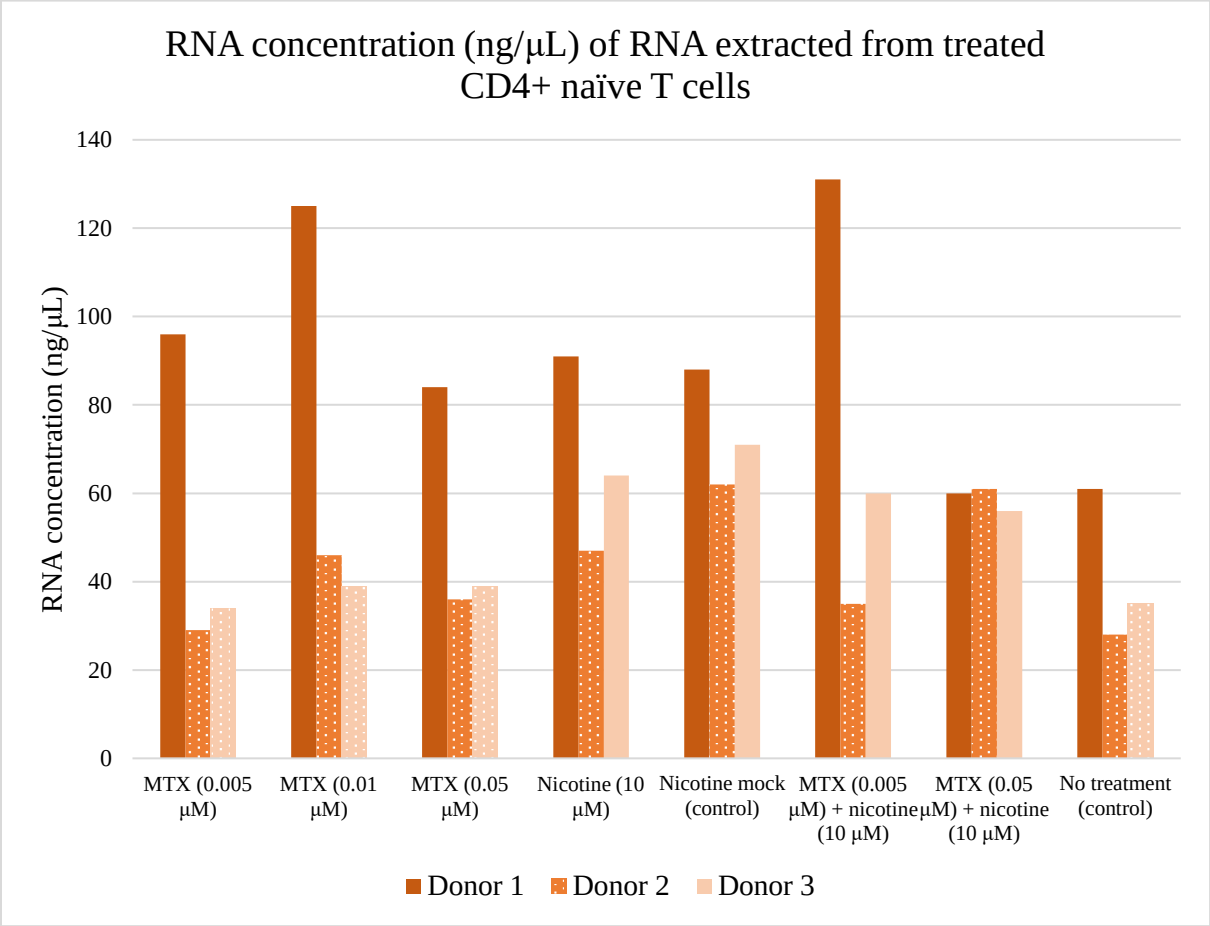

Figure 4.15: Concentrations (ng/µL) of extracted RNA. RNA concentration from treated $CD4^+$ naïve T cells, from three different donors. The RNA concentrations ranging from 28 to 131 ng/µL, were acquired using the 2100 Bioanalyzer. The dotted bars are samples that were washed an additional three times, while the non-dotted bars were washed once.

5 Discussion

In order to enable future studies to explore the effect of MTX and nicotine on $CD4^+$ naïve T cells, an optimized cultivation procedure was established, and treatments of interest determined. The chosen treatment conditions of interest were 0.005 μM, 0.01 μM and 0.05 μM of MTX, due to the relative cell proliferation of approximately 100%, 60% and 40%, respectively, and 10 μM of nicotine due to the relative cell proliferation of 100% and based on a previous work carried out on $CD8^+$ T cells exposed to nicotine (63).

5.1 Optimization of cell culture protocol

5.1.1 Activator selection

The CD3/CD28 T Cell Activator was chosen over the CD3/CD28/CD2 T Cell Activator because the cells had greater viability and a higher cell count. As this was already assessed in the first experiment, no further replicates of this experiment were performed, and the chosen activator was used for all further experiments. There could be several reasons as to why the viability and cell count was higher for this activator. Firstly, the uncertainty of the viability measurements and cell numbers should be taken into consideration, and secondly, there are biological conditions that could have influenced the differences in viability and cell counts.

There was a significant difference in viability when the T cells were treated with the different activators. The viability of 90.8% and cell count of $2.2x10^5$ cells/mL on day 5 of cell cultivation for cells treated with CD3/CD28/CD2 seemed unfavorable when compared to the viability of 97.4% and cell count of $4.2x10^5$ cells/mL of cells treated with CD3/CD28. However, the results obtained by the NucleoCounter®, used to count the cells and calculate viability, does deviate between triplicate replicate samples, from what should be a homogenous cell suspension. As there was some variance when using the instrument, the measurements cannot be considered entirely accurate. For example, the average cell counts for the CD3/CD28/CD2 activator was 7.7×10^5 cells/mL with a standard deviation of 7.1×10^4 cells/mL, which represents a discrepancy of approximately 10%. Another consideration is the risk of the cell suspension not being completely homogenous when it was divided into the two flasks on day 0 of cell cultivation. If there was a difference in number of cells in each flask from day 0, it would have exponentially affected the cell proliferation in each flask with each passing day.

There is likely, however, biological reasons as to why the viability and cell counts differs between the two activators. CD3 and CD28 provide important signals that stimulate T cell expansion when culturing $CD4^+$ T cells *in vitro* (40). According to a study carried out on T cells, adding CD2 to the T cell culture could stimulate T cell expansion as well as reduce the threshold for T cell activation (64), although this might not necessarily apply for the naïve subtype specifically. It did not seem that the anti-human CD2 monospecific antibody complex included in the CD3/CD28/CD2 activator had a positive effect on the viability or expansion of the naïve cells. Research suggests that when CD2 monoclonal antibodies are added to T cell culture, the CD2 does in fact bind to $CD45RA^+$ (naïve) T cells, however it does not facilitate in inducing cell proliferation (65). $CD45RO^+$ (memory) cells on the other hand, respond well to the CD2 antibody, suggesting that the CD2 pathway is utilized more effectively in memory cells than in naïve cells (65). CD2 is also commonly used as a surface marker for memory cells, as it is more highly expressed on memory cells than on naïve cells (66). As the $CD4^+$ T cells had already been negatively selected into a naïve T cell population when being treated with the different activators, the additional CD2 might not have had any function or could have even promoted the conversion of naïve cells to memory cells. Although, there is nothing to indicate that CD2 should affect the viability of naïve $CD4^+$ T cells negatively.

Due to lack of replicates for this experiment, it would be difficult to conclude that this activator would be the most suitable choice for future cultivation of $CD4^+$ naïve T cells. The activators were evaluated on a cell population of already isolated naïve cells. However, we decided later in the cell cultivation optimization process that the naïve population were to be isolated as a last step of the protocol. It would be interesting to see if the results were the same if the activators were compared when used on total $CD4^+$ T cells before isolation of the naïve population. A comparison of the purity of both samples using flow cytometry could also have given a better insight of the ratio of subtypes in the samples, since the naïve subtype was of interest. The viability of both cell populations was relatively high and in accordance with STEMCELL Technologies Optimization of Human T Cell Expansion Protocol: Effects of early Cell Dilution (67), with both populations having a cell viability > 90% on day 5. This indicates that using either activator for future experiments could potentially have been acceptable. More replicates of this experiment would be necessary in order to confirm that the CD3/CD28 T cell activator is in fact better suited for cultivating $CD4^+$ naïve T cells, in regard to viability and cell expansion.

5.1.2 Assessing cell viability

The viability of the $CD4^+$ T cells was predominantly based on total and non-viable cell counts obtained from the NucleoCounter®. Although AnnexinV was used to detect cells in early apoptosis during flow cytometry, the results indicated that nearly all cells were apoptotic even on day 0 of cell cultivation. This made it difficult to do any viability assessments based on the AnnexinV data from the flow analysis. The reason behind this is unknown, but while it could be because the cells are indeed in the early phase of apoptosis, the viability of the cells were >90% even on day 7 when using NucleoCounter®, so we concluded it was likely a false positive. This is not at all unlikely, as this has been shown to be the case in a previous study, where AnnexinV/PI led to a number of false positives up to 40% (58). Further, while phosphatidylserine is expressed on the cell surface on early apoptotic cells, it has also been shown to be expressed on the cell surface during activation of $CD8^+$ T cells and is suggested to occur similarly in activated $CD4^+$ T cells (68-70). This, in combination with the high false positive rate, is the likely cause for the extremely high positive AnnexinV binding, and is thus not the best assay for analyzing cell death in these cells. The AnnexinV assay is commonly performed in combination with PI to obtain a full overview of dying cells in a sample, which was not included in our analysis. PI is a simple DNA intercalator and a commonly used live/dead marker in flow cytometry, so this marker could be considered instead of AnnexinV in future experiments. However, the NucleoCounter® was therefore used as the main instrument to assess viability of the cell samples in these experiments.

5.1.3 Autofluorescence affecting cellular purity data

The purity of the $CD4^+$ T cells regarding expression of CD3 and CD8 in the samples was assessed using flow cytometry. Expectedly, CD8 was not noticeably expressed in any samples, however a population of CD3 cells were expressed in most of the cell samples analyzed. There could be a technical reason as to why the CD3 cells were detected, as described above, the isolation process of $CD4^+$ T cells does not result in a 100% pure population of naïve cells. Although, if this was the case, it would have been expected that some $CD8^+$ cells would have also been detected. A more likely theory is that the PE fluorophore on CD3 is bleeding into the detection of FITC fluorophore on CD4, and vice versa, resulting in autofluorescence during the flow analysis. Looking at the Ex/Em spectra for both fluorophores (Figure 5.1), it is clear that there is some degree of cross pollination between the two fluorophores. Both are excited by the 488nm laser, and both have some degree of emission in the corresponding filter window for the

other fluorophore. As such, the detected $CD3^+$ T cells observed, could also be highly fluorescent $CD4^+$ FITC cells.

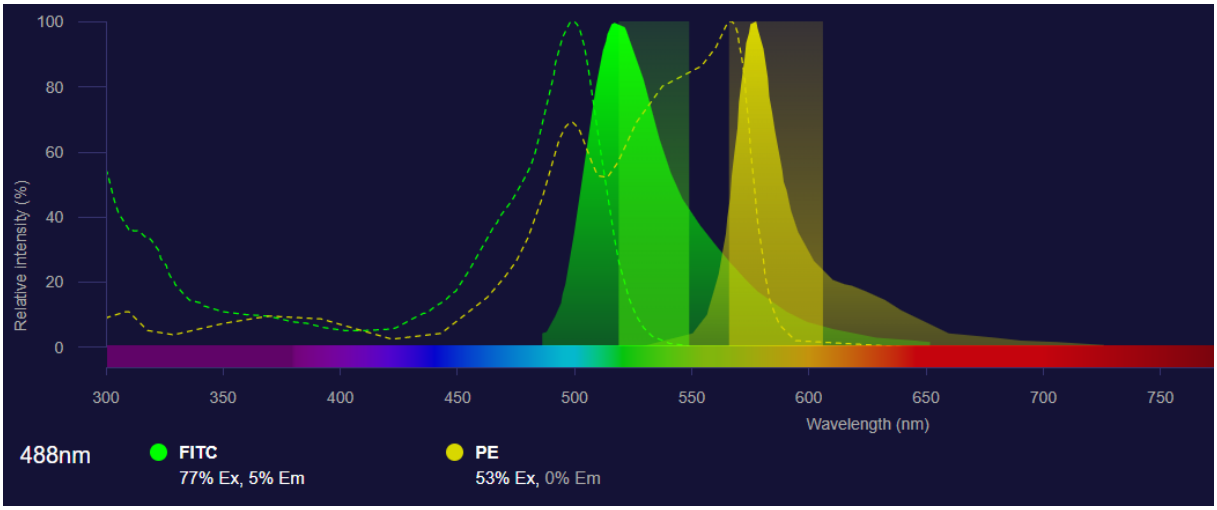

Figure 5.1: The fluorescent spectra for excitation and emission of both FITC and PE. Filters for detection of FITC (533/30) and PE (585/40) emission are plotted. The 488nm laser was used to excite both fluorophores. The emission spectra also overlap in the defined capture filters for each fluorophore, so it is expected that there will be some degree of bleeding into the opposing channels. The figure is taken from Thermo Fisher Scientific Fluorescence SpectraViewer (71).

5.1.4 Changes in the morphology of the $CD4^+$ T cell suspension culture over time

It was observed that the $CD4^+$ naïve T cell population aggregated into clusters of cells over time. Cells were therefore resuspended to loosen up the clusters of cells, which increased the homogeneity of the cell suspension. T cell clustering is normal as they are not adherent cells but suspension cells, and suspension cells often attach to each other when they reach confluency (72). T cells have been reported to reach peak clustering on day 7, and the clusters of cells will begin to decrease henceforth (73). The longest amount of time the cells were cultivated for during the cultivation process was 7 days, which correlates with this study as none of the clusters appeared to decrease in this timeframe. The morphology of the $CD4^+$ T cell population also resemble the clusters presented by STEMCELL Technologies using the same activator and media (62). T cells cluster together upon activation with CD3, CD28 and IL-2, indicating that the naïve T cells had already started to differentiate into active T cells (73). It would be interesting to see how the morphology and clustering behavior changes within this cultivation process for time periods beyond day 7, however being able to control the naïve to memory cell ratio would be problematic.

The cells were also resuspended to loosen attached cells from the plastic of the flasks and microplates used during the cultivation process. As T cells are non-adherent cells, it was not expected that the cells would adhere to the plastic, however there could have been monocytes left in the cell sample after isolation from the PBMCs. When culturing cells, monocytes tend to adhere to the plastic of wells and flasks (74), which would offer a simple explanation. However, as CD68 is used as a selective marker for monocytes and macrophages (75), it was therefore included during flow cytometry analysis and revealed no monocytes were present. As such, it is likely that the adhered cells could be $CD4^+$ T cells that had sedimented to the bottom of the wells and flasks, as the cells were also loosened by gentle agitation. Potentially using plasticware specific for culturing of suspension cells could be a possible improvement for future work with this cultivation process.

5.1.5 Expression level alteration from $CD45RA^+$ to $CD45RO^+$

Upon examination of the purity of $CD4^+$ naïve T cells using flow cytometry, it was discovered that the majority of naïve cells develop into memory cells. The proportion of cells with the $CD45RO^+$ cell surface marker for memory/activated T cells increased over time. As the focus of interest for this thesis was to examine the naïve subpopulation, this posed a challenge. This change in phenotype resulted in having to compress the cell cultivation process from 7 days, as was originally planned, into 2 days. The naïve cells were also separated from the samples as a final step of cultivation as opposed to isolation on day 0 as originally planned. Alteration of the CD45 phenotype from CD45RA to CD45RO has previously been observed (76). After 7 days of $CD4^+$ T cell cultivation, almost a complete loss of the $CD45RA^+$ population was reported, from approximately between 10-45% on day 0 to essentially 0% on day 7. This study was carried out on cells collected from HIV patients, but the results were the same for the healthy controls. The suggested reason behind this loss was that cells had been activated *in vitro*. Another study supports these findings, where over half of the population of $CD4^+$ T cells lost the $CD45RA^+$ marker at day 4, and almost completely by day 10 (77). This is also in accordance with STEMCELLS Human T Cell Expansion Protocol, which shows that after 3 days of culturing cells using the conditions described in this thesis, the majority (90%) of the T cell population will develop into memory cells. The IL-2 cytokine, included as a cofactor in the culture media, is also recognized for playing a part in the change of the CD45 phenotypes (78). IL-2 promotes the transition from the CD45RA to the CD45RO phenotype, and an increase of IL-2 concentration can increase the transition. IL-2 is also a mediator in the of CD45RO

expression after stimulation of the TCR/CD3 complex (78). As IL-2 is recommended for T cell culture (45, 67), it is a difficult task to maintain a pure naïve $CD45RA^+CD45RO^-$ T cell population during cultivation.

The majority of the cells possessed both cell surface markers, making them double positive for $CD45RA^+CD45RO^+$. The cell surface markers represent cells at different stages, as $CD45RA^+$ T cells are immature cells and $CD45RO^+$ cells are mature cells. The double positives indicate that the cells are in an intermediate phase, in the process of switching from naïve to memory (79). After naïve T cells are stimulated *in vitro*, the cells will begin to lose the expression of CD45RA and gain expression of CD45RO, with a transitional stage where both will be expressed (35). In an attempt to expand the cell population and increase proliferation of the $CD4^+$ naïve T cells using an activator, the T cells could have become too activated and initiated differentiation of the cells. $CD45RO^+$ memory cells also require less stimulation to proliferate, in comparison to $CD45RA^+$ naïve cells for patients with RA (37). With the naïve subpopulation isolated, and treated with MTX and nicotine, the cells might behave in another way than in culture with cells in other cell stages. Memory cells that have developed during *in vitro* cultivation of the cells, have not yet encountered an antigen and therefore should potentially be referred to as activated cells and not memory cells. However, since CD45RO was used as a surface marker for both activated and memory cells, it would be difficult to distinguish between memory cells already present in the sample and newly activated cells. Both memory and activated T cells were therefore termed memory cells or $CD45RO^+$ cells in this thesis.

5.2 Treatment conditions for $CD4^+$ naïve T cells as established by relative cell proliferation

5.2.1 Incubation time with cell proliferation agent WST-1

It was observed that the relative cell proliferation across the tested MTX and nicotine concentrations varied more for the 30-minute incubation with WST-1 than for the 60- and 90-minute incubations. The appropriate incubation time with WST-1 depends on the cell type and the individual experimental setup (80). In similar studies on T cells, the incubation time with WST-1 has been 2 hours or more (81, 82), indicating that the cell proliferation agent WST-1 would likely need more than 30 minutes to affect the whole sample. To be sure that the relative cell proliferation would not continue to change after 90 minutes, additional timepoints up to 4 hours were included for the further experiments. However, no additional changes were noted

after 90 minutes of WST-1 incubation, so 60- to 90-minutes should be sufficient in order to obtain results from the WST-1 assay in this cell cultivation process.

5.2.2 Final concentrations

The chosen MTX concentrations were 0.005 μM, 0.01 μM and 0.05 μM, giving approximately 40%, 60% and 100% relative cell proliferation respectively. The highest MTX concentration tested was 5 μM, however it did not offer better cellular response than 0.05 μM. The range of MTX concentrations were difficult to determine because of lack of previously reported experiments that have examined MTX treatment of naïve $CD4^+$ T cells in relation to RA. However, some studies have explored similar concentrations of MTX for the treatment of T cells. In the first study, both $CD4^+$ and $CD8^+$ T cells were isolated from healthy controls and RA patients, then treated with 0.1 μM to 1.0 μM MTX for 24 to 48 hours (83). A range between 0.01 μM and 1 μM was also found in another study carried out on Jurkat T Lymphocytes, where cell cultures were incubated between 24 to 72 hours (84), and a third study investigated the same concentrations for Jurkat T cells and U937 monocytes (85). This indicates that the MTX concentrations of interest were not farfetched compared to previous literature. We wanted to include all three concentrations as it would be interesting to examine the very last concentration before cell proliferation dropped (0.005 μM) as well as the first sample where a decrease was seen in proliferation (0.01 μM) and a concentration where proliferation had dropped beneath 50% (0.05 μM). While these were lower than the concentrations used in previous literature, they still represented the full scope of the elicited responses seen over our MTX concentration range.

The nicotine concentration of interest was 10 μM, which was a concentration that did not affect proliferation of $CD4^+$ T cells. As it was desired to investigate the effects of nicotine on normal cells and not apoptotic cells, we wanted to select a concentration of nicotine that did not induce apoptosis and would also represent 'real world' physiology of nicotine on cells *in vivo*. The last, and the initial reason we selected this concentration, was largely to parallel a study that explored the effects of 10 μM nicotine treatment on $CD8^+$ T cells isolated from RA patients and healthy donors (63). In this study, they discovered that smokers had higher prevalence of $CD8^+$ T cells within a naïve/memory phenotype, where they concluded nicotine had a role in shifted the T cell physiology, in particular reducing PD-1 expression in a specific $CD27^+CD8^+$ naïve/memory subset. Similarly to methods in this study, it would also be beneficial to use micro-RNA analysis to understand the epigenetic changes in $CD45RA^+CD45RO^+$ DP

naïve/memory T cells in response to treatment with nicotine, and to explore how and if CD27 expression can influence naïve/memory cells in $CD4^+$ T cells.

5.4 Future perspectives

As RNA extraction was included during the cultivation process, it would allow for investigating the genotypical response of $CD4^+$ naïve T cells to treatment with MTX and exposure to nicotine in further detail. Using reverse transcription, the RNA can be synthesized into cDNA, which in turn could be used for methods such as quantitative polymerase chain reaction (qPCR), real time-qPCR, droplet digital PCR or DNA sequencing, to gather more information about the cells' response to the treatments. For example, exploring the effects of MTX and nicotine on gene expression in rheumatoid arthritis risk loci: MELL1, AFF3, REL, IL2 and STAT4. These are potential genes of interest, that have previously been identified as 5 of the 101 genes associated with the development of RA (26), and have been highlighted as potential (and current) RA targets for future therapies. Expression of CD27 and $CD45RA^+CD62L^+$ could also be interesting T cell subtypes to explore in relation to smoking and the effect of nicotine on RA development and progression (63). Understanding how expression of these genes specifically change in $CD4^+$ naïve T cells of healthy donors in response to MTX and nicotine, could give further insights to RA patient responses to MTX therapy, the impact and risk associated with cigarette smoking, and alter future approaches in developing new treatment regimens for RA.

6 Conclusion

The aim of this project was to optimize a $CD4^+$ T cell cultivation protocol in order to further study the cells' response to treatment with MTX and exposure to nicotine. It has been assessed what activator was optimal for this purpose, by comparing viability and cell counts of two activators containing different combinations of stimulants. Furthermore, the optimal cultivation time before the cells start to change morphology, phenotype and the viability decrease, has been evaluated. It has also been established concentrations of MTX and nicotine that could be of interest for future studies, in regards to RA treatment. However, more research is required to investigate the cellular responses to the treatment with MTX and exposure to nicotine.

References

1. Chaplin DD. Overview of the immune response. J Allergy Clin Immunol. 2010;125(2 Suppl 2):S3-S23.

2. Delves PJ, Roitt IM. The Immune System. New England Journal of Medicine. 2000;343(1):37-49.

3. Elliott DE, Siddique SS, Weinstock JV. Innate immunity in disease. Clin Gastroenterol Hepatol. 2014;12(5):749-55.

4. Luckheeram RV, Zhou R, Verma AD, Xia B. $CD4^+$T cells: differentiation and functions. Clin Dev Immunol. 2012;2012:925135-.

5. Alberts B, Johnson AD, Lewis J, Morgan D, Raff M, Roberts K, et al. Molecular Biology of the Cell. 6th ed. New York and Abingdon, UK: Garland Science; 2014.

6. Kumar BV, Connors TJ, Farber DL. Human T Cell Development, Localization, and Function throughout Life. Immunity. 2018;48(2):202-13.

7. Takahama Y. Journey through the thymus: stromal guides for T-cell development and selection. Nature Reviews Immunology. 2006;6(2):127-35.

8. Shah DK. T-cell development in thymus. British Society for Immunology. Accessed on May 2022.

9. Klein L, Kyewski B, Allen PM, Hogquist KA. Positive and negative selection of the T cell repertoire: what thymocytes see (and don't see). Nat Rev Immunol. 2014;14(6):377-91.

10. Gaudino SJ, Kumar P. Cross-Talk Between Antigen Presenting Cells and T Cells Impacts Intestinal Homeostasis, Bacterial Infections, and Tumorigenesis. Front Immunol. 2019;10:360-.

11. Bustin S. Molecular Biology of the Cell, Sixth Edition; ISBN: 9780815344643; and Molecular Biology of the Cell, Sixth Edition, The Problems Book; ISBN 9780815344537. Int J Mol Sci. 2015;16(12):28123-5.

12. Elgueta R, Benson MJ, de Vries VC, Wasiuk A, Guo Y, Noelle RJ. Molecular mechanism and function of CD40/CD40L engagement in the immune system. Immunol Rev. 2009;229(1):152-72.

13. Couture A, Garnier A, Docagne F, Boyer O, Vivien D, Le-Mauff B, et al. HLA-Class II Artificial Antigen Presenting Cells in CD4+ T Cell-Based Immunotherapy. Front Immunol. 2019;10.

14. Sckisel GD, Bouchlaka MN, Monjazeb AM, Crittenden M, Curti BD, Wilkins DE, et al. Out-of-Sequence Signal 3 Paralyzes Primary CD4(+) T-Cell-Dependent Immunity. Immunity. 2015;43(2):240-50.

15. Brahmakshatriya V, Kuang Y, Devarajan P, Xia J, Zhang W, Vong AM, et al. IL-6 Production by TLR-Activated APC Broadly Enhances Aged Cognate CD4 Helper and B Cell Antibody Responses In Vivo. J Immunol. 2017;198(7):2819-33.

16. Zhang N, Bevan Michael J. CD8+ T Cells: Foot Soldiers of the Immune System. Immunity. 2011;35(2):161-8.

17. Mittrücker H-W, Visekruna A, Huber M. Heterogeneity in the Differentiation and Function of CD8+ T Cells. Archivum Immunologiae et Therapiae Experimentalis. 2014;62(6):449-58.

18. Golubovskaya V, Wu L. Different Subsets of T Cells, Memory, Effector Functions, and CAR-T Immunotherapy. Cancers (Basel). 2016;8(3):36.

19. Rocamora-Reverte L, Melzer FL, Würzner R, Weinberger B. The Complex Role of Regulatory T Cells in Immunity and Aging. Front Immunol. 2021;11.

20. Eagar TN, Miller SD. 16 - Helper T-Cell Subsets and Control of the Inflammatory Response. In: Rich RR, Fleisher TA, Shearer WT, Schroeder HW, Frew AJ, Weyand CM, editors. Clinical Immunology (Fifth Edition). London: Elsevier; 2019. p. 235-45.e1.

21. Wang L, Wang F-S, Gershwin ME. Human autoimmune diseases: a comprehensive update. Journal of Internal Medicine. 2015;278(4):369-95.

22. Rai E, Wakeland EK. Genetic predisposition to autoimmunity – What have we learned? Seminars in Immunology. 2011;23(2):67-83.

23. Allan Gibofsky MJFF. Overview of Epidemiology, Pathophysiology, and Diagnosis of Rheumatoid Arthritis. Supplements and Featured Publications. 2012;18(13 Suppl).

24. Lin Y-J, Anzaghe M, Schülke S. Update on the Pathomechanism, Diagnosis, and Treatment Options for Rheumatoid Arthritis. Cells. 2020;9(4):880.

25. Klareskog L, Malmström V, Lundberg K, Padyukov L, Alfredsson L. Smoking, citrullination and genetic variability in the immunopathogenesis of rheumatoid arthritis. Seminars in Immunology. 2011;23(2):92-8.

26. Okada Y, Wu D, Trynka G, Raj T, Terao C, Ikari K, et al. Genetics of rheumatoid arthritis contributes to biology and drug discovery. Nature. 2014;506(7488):376-81.

27. Ngo ST, Steyn FJ, McCombe PA. Gender differences in autoimmune disease. Frontiers in Neuroendocrinology. 2014;35(3):347-69.

28. Mohammed A, Alshamarri T, Adeyeye T, Lazariu V, McNutt L-A, Carpenter DO. A comparison of risk factors for osteo- and rheumatoid arthritis using NHANES data. Preventive Medicine Reports. 2020;20:101242.

29. Sungwon R. Smoking as a Preventable Risk Factor for Rheumatoid Arthritis: Rationale for Smoking Cessation Treatment in Patients with Rheumatoid Arthritis. J Rheum Dis. 2019;26(1):12-9.

30. Chang K, Yang SM, Kim SH, Han KH, Park SJ, Shin JI. Smoking and rheumatoid arthritis. Int J Mol Sci. 2014;15(12):22279-95.

31. McHugh J. Nicotine exacerbates arthritis. Nature Reviews Rheumatology. 2017;13(3):132-.

32. McInnes IB, Schett G. The Pathogenesis of Rheumatoid Arthritis. New England Journal of Medicine. 2011;365(23):2205-19.

33. Weyand CM, Bryl E, Goronzy JJ. The role of T cells in rheumatoid arthritis. Arch Immunol Ther Exp (Warsz). 2000;48(5):429-35.

34. Yang Z, Shen Y, Oishi H, Matteson EL, Tian L, Goronzy JJ, et al. Restoring oxidant signaling suppresses proarthritogenic T cell effector functions in rheumatoid arthritis. Sci Transl Med. 2016;8(331):331ra38-ra38.

35. Summers KL, O'Donnell JL, Hart DN. Co-expression of the CD45RA and CD45RO antigens on T lymphocytes in chronic arthritis. Clin Exp Immunol. 1994;97(1):39-44.

36. Mellado M, Martínez-Muñoz L, Cascio G, Lucas P, Pablos JL, Rodríguez-Frade JM. T Cell Migration in Rheumatoid Arthritis. Front Immunol. 2015;6:384-.

37. Ponchel F, Morgan AW, Bingham SJ, Quinn M, Buch M, Verburg RJ, et al. Dysregulated lymphocyte proliferation and differentiation in patients with rheumatoid arthritis. Blood. 2002;100(13):4550-6.

38. Dittel BN. CD4 T cells: Balancing the coming and going of autoimmune-mediated inflammation in the CNS. Brain, Behavior, and Immunity. 2008;22(4):421-30.

39. Friedman B, Cronstein B. Methotrexate mechanism in treatment of rheumatoid arthritis. Joint Bone Spine. 2019;86(3):301-7.

40. Trickett A, Kwan YL. T cell stimulation and expansion using anti-CD3/CD28 beads. Journal of Immunological Methods. 2003;275(1):251-5.

41. Jiao J, Zhao X, Hou R, Wang Y, Chang W, Liang N, et al. Comparison of two commonly used methods for stimulating T cells. Biotechnology Letters. 2019;41(12):1361-71.

42. Xia F, Qian C-R, Xun Z, Hamon Y, Sartre A-M, Formisano A, et al. TCR and CD28 Concomitant Stimulation Elicits a Distinctive Calcium Response in Naive T Cells. Front Immunol. 2018;9.

43. Alegre M-L, Thompson CB, Gajewski TF. Second Signals for Lymphocyte Activation. In: Delves PJ, editor. Encyclopedia of Immunology (Second Edition). Oxford: Elsevier; 1998. p. 2145-51.

44. Nurieva R, Thomas S, Nguyen T, Martin-Orozco N, Wang Y, Kaja M-K, et al. T-cell tolerance or function is determined by combinatorial costimulatory signals. The EMBO Journal. 2006;25(11):2623-33.

45. Bachmann MF, Oxenius A. Interleukin 2: from immunostimulation to immunoregulation and back again. EMBO Rep. 2007;8(12):1142-8.

46. Medvec AR, Ecker C, Kong H, Winters EA, Glover J, Varela-Rohena A, et al. Improved Expansion and In Vivo Function of Patient T Cells by a Serum-free Medium. Mol Ther Methods Clin Dev. 2017;8:65-74.

47. Li F-Y, Chaigne-Delalande B, Kanellopoulou C, Davis JC, Matthews HF, Douek DC, et al. Second messenger role for Mg2+ revealed by human T-cell immunodeficiency. Nature. 2011;475(7357):471-6.

48. Mulcahy MJ, Lester HA. Granulocytes as models for human protein marker identification following nicotine exposure. J Neurochem. 2017;142 Suppl 2(Suppl 2):151-61.

49. Sutton DW, Chen PC, Schmid-Schönbein GW. Cell separation in the buffy coat. Biorheology. 1988;25(4):663-73.

50. Bittersohl H, Steimer W. Chapter 9 - Intracellular concentrations of immunosuppressants. In: Oellerich M, Dasgupta A, editors. Personalized Immunosuppression in Transplantation. San Diego: Elsevier; 2016. p. 199-226.

51. Thiel A, Scheffold A, Radbruch A. Immunomagnetic cell sorting—pushing the limits. Immunotechnology. 1998;4(2):89-96.

52. Le Dieu R, Taussig D, Lister TA, Gribben JG. Negative immunomagnetic selection of T cells from peripheral blood of presentation AML specimens. Journal of Immunological Methods. 2009;348(1):95-100.

53. Cadena-Herrera D, Esparza-De Lara JE, Ramírez-Ibañez ND, López-Morales CA, Pérez NO, Flores-Ortiz LF, et al. Validation of three viable-cell counting methods: Manual, semi-automated, and automated. Biotechnol Rep (Amst). 2015;7:9-16.

54. Shah D, Naciri M, Clee P, Al-Rubeai M. NucleoCounter—An efficient technique for the determination of cell number and viability in animal cell culture processes. Cytotechnology. 2006;51(1):39-44.

55. McKinnon KM. Flow Cytometry: An Overview. Curr Protoc Immunol. 2018;120:5.1.-5.1.11.

56. Feher K, Kirsch J, Radbruch A, Chang H-D, Kaiser T. Cell population identification using fluorescence-minus-one controls with a one-class classifying algorithm. Bioinformatics. 2014;30(23):3372-8.

57. Bendall LJ, Green DR. Autopsy of a cell. Leukemia. 2014;28(6):1341-3.

58. Rieger AM, Nelson KL, Konowalchuk JD, Barreda DR. Modified annexin V/propidium iodide apoptosis assay for accurate assessment of cell death. J Vis Exp. 2011(50):2597.

59. Kamiloglu S, Sari G, Ozdal T, Capanoglu E. Guidelines for cell viability assays. Food Frontiers. 2020;1(3):332-49.

60. Larramendy M, Soloneski S. Genotoxicity: A Predictable Risk to Our Actual World: IntechOpen; 2018.

61. s.n. Protocol Guide: WST-1 Assay for Cell Proliferation and Viability Sigma Aldrich Sigma Aldrich Accessed in May 2022 [Available from: https://www.sigmaaldrich.com/NO/en/technical-documents/protocol/cell-culture-and-cell-culture-analysis/cell-counting-and-health-analysis/cell-proliferation-reagent-wst-1.

62. s.n. ImmunoCult™ Human CD3/CD28 T Cell Activator. Accessed in May 2022.

63. Wasén C, Ospelt C, Camponeschi A, Erlandsson MC, Andersson KME, Silfverswärd ST, et al. Nicotine Changes the microRNA Profile to Regulate the FOXO Memory Program of CD8+ T Cells in Rheumatoid Arthritis. Front Immunol. 2020;11.

64. Gollob JA, Li J, Reinherz EL, Ritz J. CD2 regulates responsiveness of activated T cells to interleukin 12. J Exp Med. 1995;182(3):721-31.

65. Wallace DL, Beverley PC. Phenotypic changes associated with activation of CD45RA+ and CD45RO+ T cells. Immunology. 1990;69(3):460-7.

66. Binder C, Cvetkovski F, Sellberg F, Berg S, Paternina Visbal H, Sachs DH, et al. CD2 Immunobiology. Front Immunol. 2020;11.

67. s.n. Optimization of Human T Cell Expansion Protocol: Effects of Early Cell Dilution STEMCELL Technologies Accessed in May 2022 [Available from:

https://www.stemcell.com/optimization-of-human-t-cell-expansion-protocol-effects-of-early-cell-dilution.html.

68. MacDonald A, Lam B, Lin J, Ferrall L, Kung YJ, Tsai YC, et al. Delivery of IL-2 to the T Cell Surface Through Phosphatidylserine Permits Robust Expansion of CD8 T Cells. Front Immunol. 2021;12.

69. Fischer K, Voelkl S, Berger J, Andreesen R, Pomorski T, Mackensen A. Antigen recognition induces phosphatidylserine exposure on the cell surface of human CD8+ T cells. Blood. 2006;108(13):4094-101.

70. Elliott JI, Surprenant A, Marelli-Berg FM, Cooper JC, Cassady-Cain RL, Wooding C, et al. Membrane phosphatidylserine distribution as a non-apoptotic signalling mechanism in lymphocytes. Nature Cell Biology. 2005;7(8):808-16.

71. s.n. Fluorescence SpectraViewer Thermo Fisher Scientific Accessed May 2022 [Available from: https://www.thermofisher.com/order/fluorescence-spectraviewer#!/.

72. s.n. Guidelines to Maintain Cultured Cells Thermo Fisher ScientificAccessed in May 2022 [Available from: https://www.thermofisher.com/no/en/home/references/gibco-cell-culture-basics/cell-culture-protocols/maintaining-cultured-cells.html.

73. Li M, Chin L-Y, Shukor S, Tamayo AG, Maus MV, Parekkadan B. Effects of intermittent T-cell cluster disaggregation on proliferative capacity and checkpoint marker expression. Autoimmunity. 2019;52(3):102-7.

74. Liu H, Shi B, Huang C-C, Eksarko P, Pope RM. Transcriptional diversity during monocyte to macrophage differentiation. Immunol Lett. 2008;117(1):70-80.

75. Klinder A, Markhoff J, Jonitz-Heincke A, Sterna P, Salamon A, Bader R. Comparison of different cell culture plates for the enrichment of non-adherent human mononuclear cells. Exp Ther Med. 2019;17(3):2004-12.

76. Pinto L, Covas MJ, Victorino RM. Loss of CD45RA and gain of CD45RO after in vitro activation of lymphocytes from HIV-infected patients. Immunology. 1991;73(2):147-50.

77. Early E, Reen DJ. Rapid conversion of naive to effector T cell function counteracts diminished primary human newborn T cell responses. Clin Exp Immunol. 1999;116(3):527-33.

78. Roth MD. Interleukin 2 induces the expression of CD45RO and the memory phenotype by CD45RA+ peripheral blood lymphocytes. J Exp Med. 1994;179(3):857-64.

79. Wallace DL, Beverley PC. Phenotypic changes associated with activation of CD45RA+ and CD45RO+ T cells. Immunology. 1990;69(3):460-7.

80. s.n. Cell Proliferation Reagent WST-1 Sigma-Aldrich, Roche Accessed in May 2022 [Available from: https://www.sigmaaldrich.com/deepweb/assets/sigmaaldrich/product/documents/350/519/cellprorobul.pdf

81. Van Belle K, Herman J, Boon L, Waer M, Sprangers B, Louat T. Comparative In Vitro Immune Stimulation Analysis of Primary Human B Cells and B Cell Lines. Journal of Immunology Research. 2016;2016:5281823.

82. Koyanagi M, Kawakabe S, Arimura Y. A comparative study of colorimetric cell proliferation assays in immune cells. Cytotechnology. 2016;68(4):1489-98.

83. Spurlock CF, 3rd, Aune ZT, Tossberg JT, Collins PL, Aune JP, Huston JW, 3rd, et al. Increased sensitivity to apoptosis induced by methotrexate is mediated by JNK. Arthritis Rheum. 2011;63(9):2606-16.

84. Spurlock CF, 3rd, Tossberg JT, Fuchs HA, Olsen NJ, Aune TM. Methotrexate increases expression of cell cycle checkpoint genes via JNK activation. Arthritis Rheum. 2012;64(6):1780-9.

85. Olsen NJ, Spurlock CF, 3rd, Aune TM. Methotrexate induces production of IL-1 and IL-6 in the monocytic cell line U937. Arthritis Res Ther. 2014;16(1):R17-R.

Appendix I

Includes kits, reagents, equipment, instruments, and software used in this thesis, in the respected order.

Table S1: Kits with corresponding supplier, country, and catalog number.

Kits	Supplier	Country	Cat. No.
EasySep™ Human CD4+ T Cell Isolation Kit	STEMCELL™ Technologies	Canada	17952
EasySep™ Human Pan-CD25 Positive Selection and Depletion Kit	STEMCELL™ Technologies	Canada	17861
EasySep™ Human PE Positive Selection Kit II	STEMCELL™ Technologies	Canada	17664
PE anti-human CD45RO Antibody	BioLegend®	USA	304206
RNA 6000 Nano kit	Agilent Technologies	USA	5067-1511
RNA/DNA/Protein Purification Plus Kit	Norgen Biotek Corp.	Canada	47700

Table S2: Reagents with corresponding supplier, country, and catalog number.

Reagents	Supplier	Country	Cat. No.
(−)-Nicotine, ≥99% (GC), liquid (5 mL)	Sigma-Aldrich	Germany	N3876-5mL
10xAnnexin V Binding Buffer	BD Biosciences	USA	51-66121E
Absolutt alkohol prima (99.9%)	KiiLTO	Norway	600068
Cell Proliferation Reagent WST-1	Roche Diagnostics	Germany	11644807001
EDTA (0.5M, pH = 8)	Thermo Fisher Scientific	USA	AM9262
Fetal Bovine Serum	BIOWEST	France	Unknown
FITC Annexin V	BD Biosciences	USA	556419
Gibco™ DPBS	Thermo Fisher Scientific	USA	14190144
Human Recombinant IL-2 (rhIL-2) Cytokine 10 ng/mL	STEMCELL Technologies	Canada	Unknown

Reagents	Supplier	Country	Cat. No.
ImmunoCult™ Human CD3/CD28 T Cell Activator	STEMCELL™ Technologies	Canada	10971
ImmunoCult™ Human CD3/CD28/CD2 T Cell Activator	STEMCELL™ Technologies	Canada	10970
ImmunoCult™-XF T Cell Expansion Medium	STEMCELL™ Technologies	Canada	10981
Lymphoprep™	STEMCELL Technologies	Canada	07811
Methotrexate Ebetrex (100 mg/mL)	EBEWE Pharma	Austria	508698
Nuclease-Free Water	Qiagen	Germany	129114
Reagent A100 Lysis Buffer	ChemoMetec	Denmark	910-0003
Reagent B Stabilizing Buffer	ChemoMetec	Denmark	910-0002
RNase Away™ Decontamination Reagent	Thermo Fisher Scientific	USA	10328011
Trypan Blue stain (0.4%)	Thermo Fisher Scientific	USA	T10282
γ-globulin	Sigma-Aldrich	USA	G4386-1G

Table S3: Equipment with corresponding supplier, country, and catalog number.

Equipment	Supplier	Country	Cat. No.
Chip Priming Station	Agilent Technologies	USA	5065-4401
Countess™ Cell Counting Chamber Slide	Thermo Fisher Scientific	USA	C10228
EasySep™ Magnet	STEMCELL™ Technologies	Canada	18000
Falcon™ 14 mL Polystyrene Round-Bottom Tube	BD Biosciences	USA	35207
Falcon™ 5 mL Polypropylene Round-Botom Tubes	Thermo Fisher Scientific	USA	352063
NucleoCassette™	ChemoMetec	Denmark	941-0001

Equipment	Supplier	Country	Cat. No.
Nunc™ EasYFlask Cell Culture Flask ($25cm^2$)	Thermo Fisher Scientific	USA	156367
Nunc™ MicroWell™ 96-Well Plates	Thermo Fisher Scientific	USA	161093
SepMate™-50 Tubes	STEMCELL™ Technologies	Canada	15450

Table S4: Instruments with corresponding supplier and country.

Instruments	Supplier	Country
2100 Bioanalyzer Instrument	Agilent Technologies	USA
BD Accuri™ C6 Plus Personal Flow Cytometer	BD Biosciences	USA
Centrifuge 5810 R	Eppendorf	Germany
Countess® II FL Automatic Cell Counter	Thermo Fisher Scientific	USA
Forma™ Steri-Cycle™ i160 CO2 Incubator, 165 L	Thermo Fisher Scientific	USA
Inverted Routine Microscope ECLIPSE Ts2	Nikon	Japan
NucleoCounter® NC100™	ChemoMetec	Denmark
STD Fume Hood	Kilab AS	Norway
Thermo Scientific™ Maxisafe 2030i Biosafety Cabinet	Thermo Fisher Scientific	USA
VersaMax Microplate Reader	Molecular Devices	USA

Table S5: Software with corresponding supplier and country.

Software	Supplier	Country
2100 Bioanalyzer Expert Software	Agilent Technologies	USA
BD Accuri™ C6 Plus Sofware	BD Biosciences	USA
Excel version 16.60	Microsoft	USA
Graphpad Prism 9	Graphpad Software, Inc.	USA
SoftMax Pro 6.4	Molecular Devices	USA

Appendix II

Initial and final 96-well plate setups for the WST-1 assay, in the respected order.

MTX concentrations

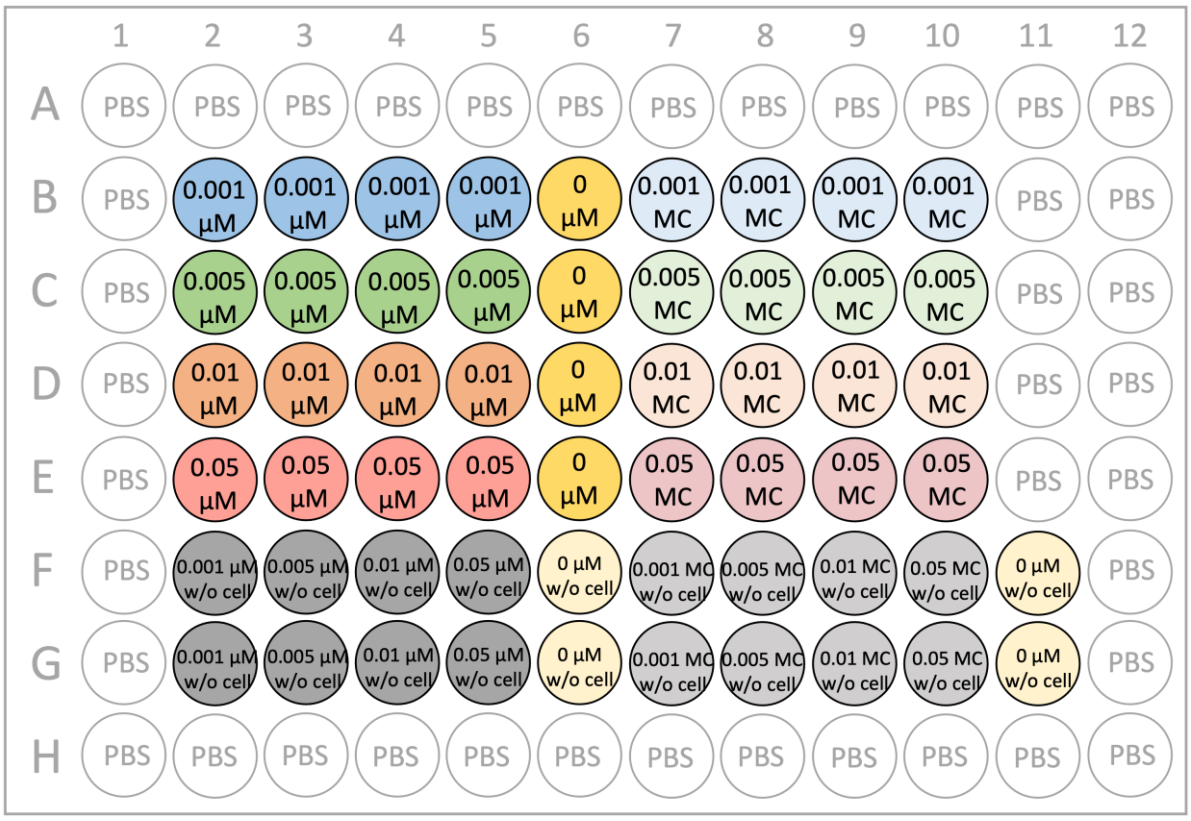

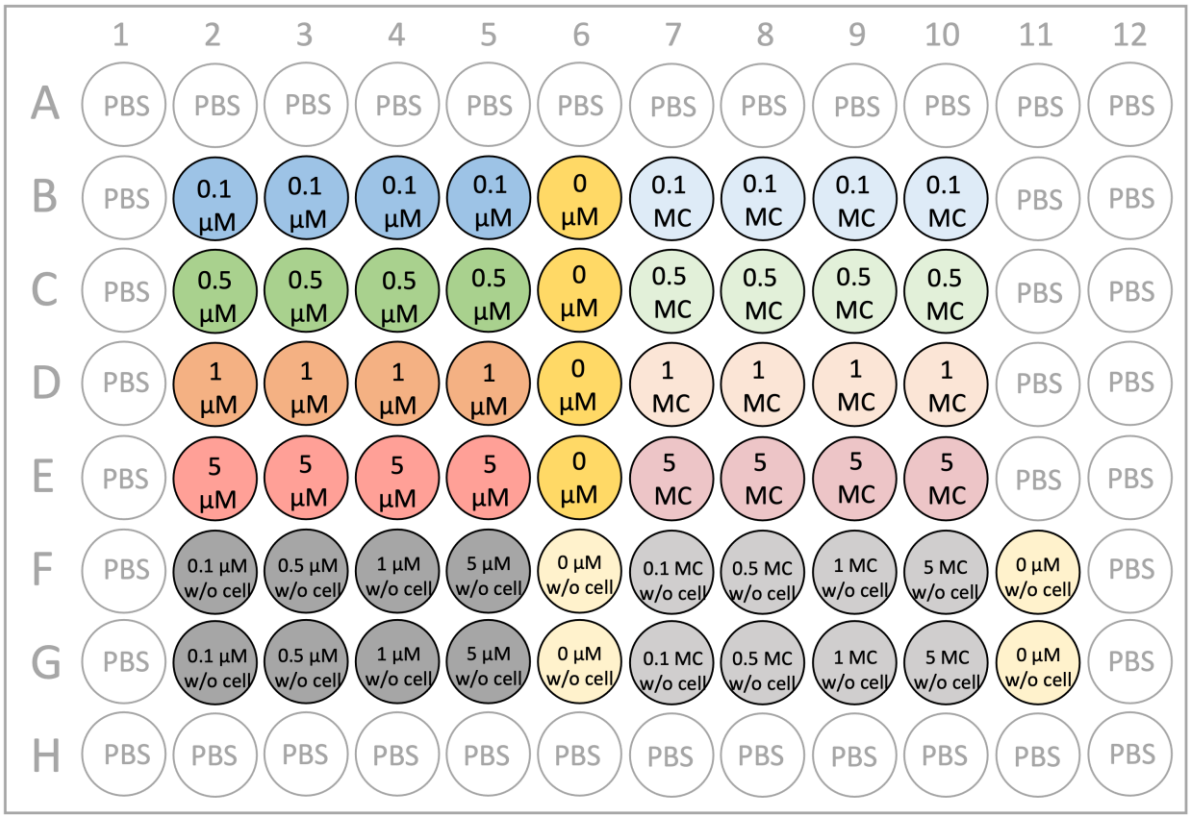

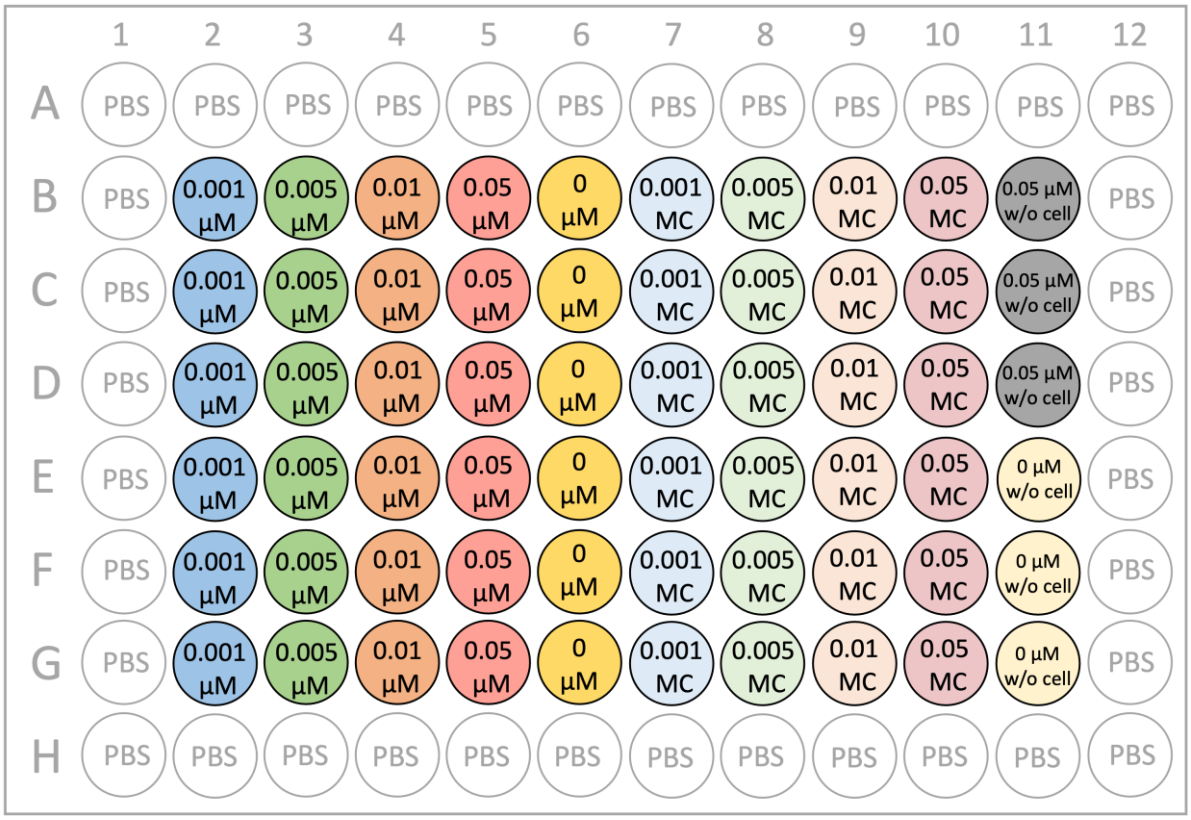
1 2 3 4 5 6 7 8 9 10 11 12
A PBS PBS PBS PBS PBS PBS PBS PBS PBS PBS PBS PBS
B PBS 0.001 µM 0.005 µM 0.01 µM 0.05 µM 0 µM 0.001 MC 0.005 MC 0.01 MC 0.05 MC 0.05 µM w/o cell PBS
C PBS 0.001 µM 0.005 µM 0.01 µM 0.05 µM 0 µM 0.001 MC 0.005 MC 0.01 MC 0.05 MC 0.05 µM w/o cell PBS
D PBS 0.001 µM 0.005 µM 0.01 µM 0.05 µM 0 µM 0.001 MC 0.005 MC 0.01 MC 0.05 MC 0.05 µM w/o cell PBS
E PBS 0.001 µM 0.005 µM 0.01 µM 0.05 µM 0 µM 0.001 MC 0.005 MC 0.01 MC 0.05 MC 0 µM w/o cell PBS
F PBS 0.001 µM 0.005 µM 0.01 µM 0.05 µM 0 µM 0.001 MC 0.005 MC 0.01 MC 0.05 MC 0 µM w/o cell PBS
G PBS 0.001 µM 0.005 µM 0.01 µM 0.05 µM 0 µM 0.001 MC 0.005 MC 0.01 MC 0.05 MC 0 µM w/o cell PBS
H PBS PBS PBS PBS PBS PBS PBS PBS PBS PBS PBS PBS

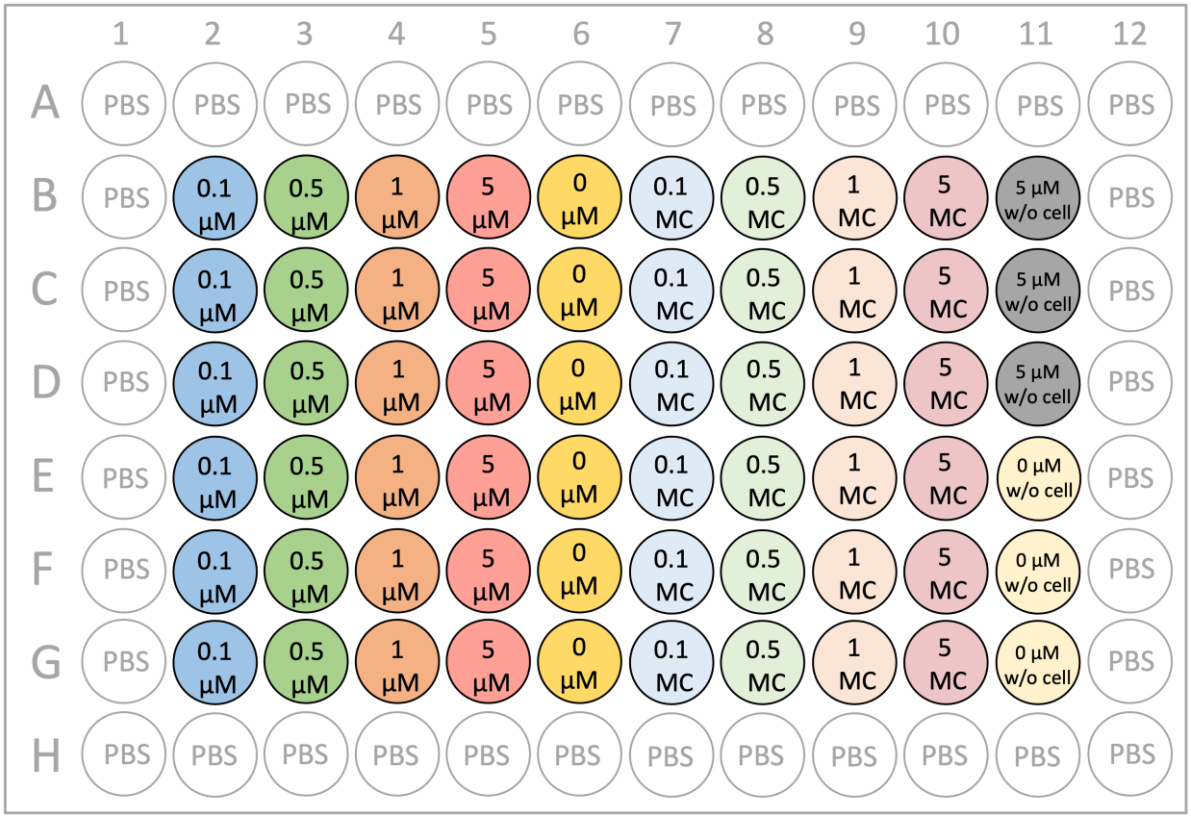
1 2 3 4 5 6 7 8 9 10 11 12
A PBS PBS PBS PBS PBS PBS PBS PBS PBS PBS PBS PBS
B PBS 0.1 µM 0.5 µM 1 µM 5 µM 0 µM 0.1 MC 0.5 MC 1 MC 5 MC 5 µM w/o cell PBS
C PBS 0.1 µM 0.5 µM 1 µM 5 µM 0 µM 0.1 MC 0.5 MC 1 MC 5 MC 5 µM w/o cell PBS
D PBS 0.1 µM 0.5 µM 1 µM 5 µM 0 µM 0.1 MC 0.5 MC 1 MC 5 MC 5 µM w/o cell PBS
E PBS 0.1 µM 0.5 µM 1 µM 5 µM 0 µM 0.1 MC 0.5 MC 1 MC 5 MC 0 µM w/o cell PBS
F PBS 0.1 µM 0.5 µM 1 µM 5 µM 0 µM 0.1 MC 0.5 MC 1 MC 5 MC 0 µM w/o cell PBS
G PBS 0.1 µM 0.5 µM 1 µM 5 µM 0 µM 0.1 MC 0.5 MC 1 MC 5 MC 0 µM w/o cell PBS
H PBS PBS PBS PBS PBS PBS PBS PBS PBS PBS PBS PBS

Nicotine concentrations

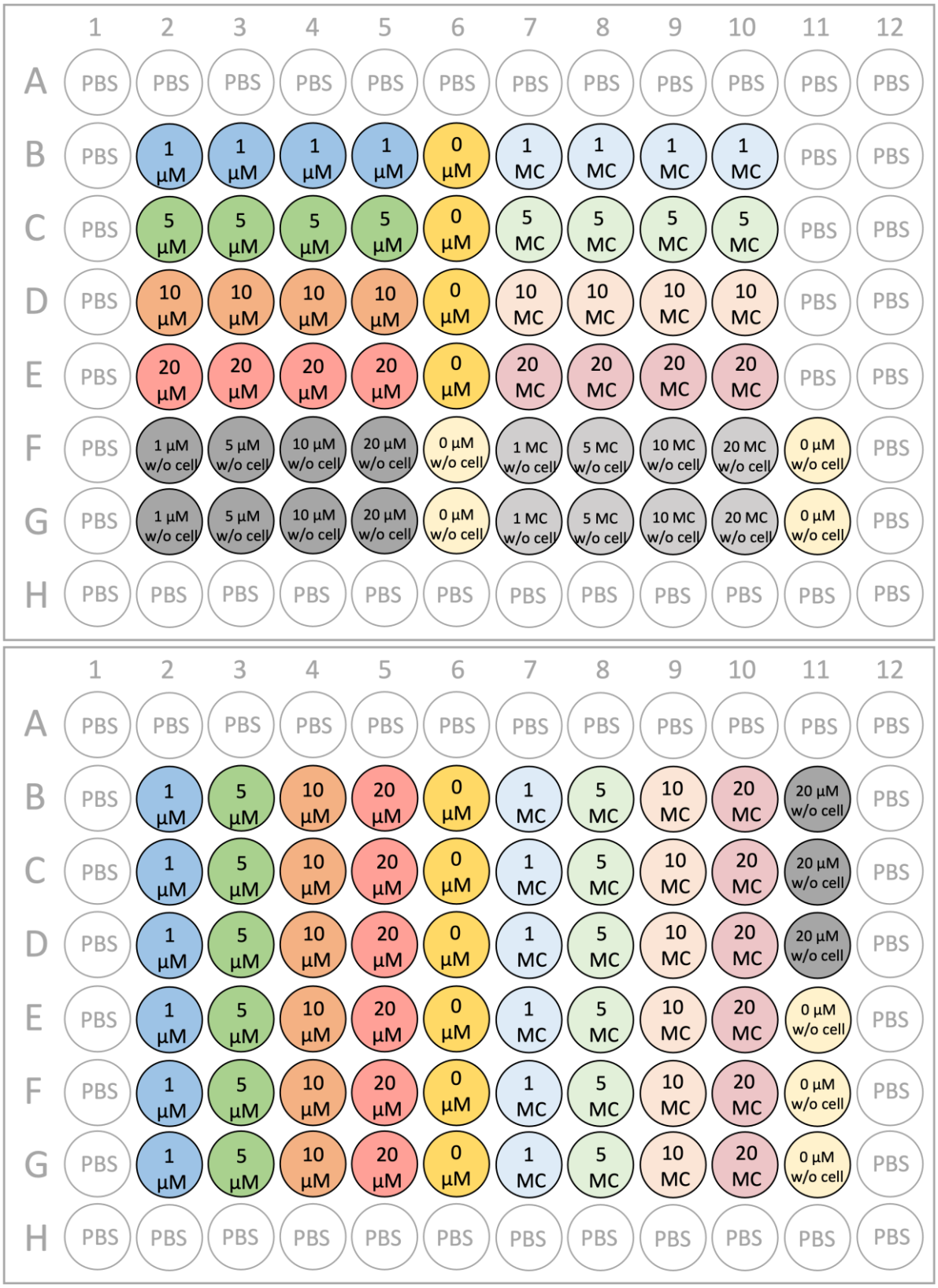

Appendix III

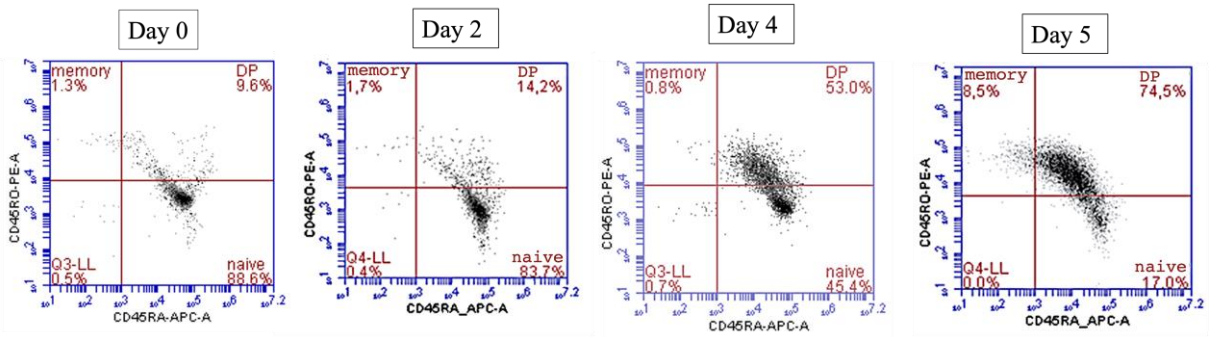

Ratio of naïve to memory T cells for day 0, day 2, day 4 and day 5 of cultivation of $CD4^+$ naïve T cells. Figure included all data from Figure 4.6B. Highlighting 2 distinct T cell populations seen on day 4: $CD45RA^+CD45RO^-$ naïve cells in the bottom right and $CD45RA^+CD45RA^+$ double positive (DP) in the top right.

Appendix IV

Mock MTX samples (i.e. parallel samples without MTX treatment) were also included in the analysis to ensure that any possible decrease in cell proliferation was not a result of media added to the wells. The data from the 48-hour MTX mock assay, did not show any decrease in cell proliferation, indicating that the MTX seems to be the major factor responsible for the decrease in cell proliferation (Figure 4.10).

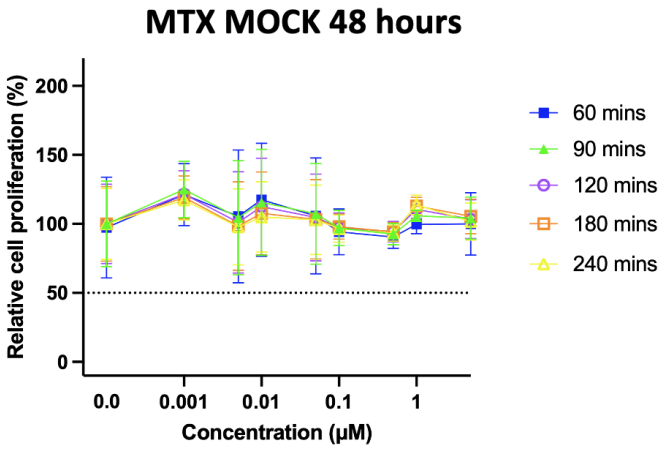

Effects of MTX mock control on relative cell proliferation of CD4$^+$ T cells. Cells were treated with additional media corresponding to the additional media used to dilute the MTX, but without any additional MTX. Relative cell proliferation was measured after 48 hours of incubation, using a WST-1 assay. The plates were incubated with WST-1 and absorbance was read at timepoints ranging from 60-240 minutes. The y-axis show the percentage of relative cell proliferation in relation to the concentration(µM) of MTX mock controls represented in the x-axis. Data is presented as the mean ± SE of every concentration performed in six replicates.

Norges miljø- og biovitenskapelig universitet
Noregs miljø- og biovitskapelege universitet
Norwegian University of Life Sciences

Postboks 5003
NO-1432 Ås
Norway